

1977

Sedimentation in reservoirs, December 1977.

Willard A. Murray

Follow this and additional works at: <http://preserve.lehigh.edu/engr-civil-environmental-fritz-lab-reports>

Recommended Citation

Murray, Willard A., "Sedimentation in reservoirs, December 1977." (1977). *Fritz Laboratory Reports*. Paper 2178.
<http://preserve.lehigh.edu/engr-civil-environmental-fritz-lab-reports/2178>

This Technical Report is brought to you for free and open access by the Civil and Environmental Engineering at Lehigh Preserve. It has been accepted for inclusion in Fritz Laboratory Reports by an authorized administrator of Lehigh Preserve. For more information, please contact preserve@lehigh.edu.

Bed Profile Prediction for Nonuniform Flow

by

David C. Beechwood

FRID. H. SILLING
LABORATORY LIBRARY

A Research Report
Presented to the Graduate Committee
of Lehigh University
in Candidacy for the Degree of
Master of Science
in
Civil Engineering

Lehigh University

1978

CERTIFICATE OF APPROVAL

This research report is accepted and approved in partial fulfillment of the requirements for the degree of Master of Science.

12/1/78
(date)

Professor in Charge

Chairman of Department

ABSTRACT

An idealized reservoir sedimentation situation with mildly nonuniform flow was studied both experimentally and analytically. A computer package to calculate sediment transport rates directly from given flow conditions, based on Einstein's 1950 bedload function, was developed. This package was utilized to predict the steady state bed profile for a laboratory reservoir. The bed profile predictions were found to correspond closely to the actual profiles observed in the laboratory. Studies concerning the variation of the bedload transport rate with distance into the reservoir were inconclusive.

ACKNOWLEDGEMENTS

The writer would like to extend his appreciation to Dr. Willard A. Murray, under whose direction and guidance this report was prepared. Mr. Elias Dittbrenner is also to be acknowledged for his assistance in the construction of the experimental apparatus.

The work upon which this report is based was supported in part by funds provided by the National Science Foundation as a portion of Fritz Engineering Laboratory Project No. 410, Reservoir Sedimentation.

TABLE OF CONTENTS

	<u>Page</u>
ABSTRACT	iii
ACKNOWLEDGEMENTS	iv
LIST OF FIGURES	
LIST OF TABLES	
1. INTRODUCTION	1
1.1 Introductory Remarks	1
1.2 Scope of the Project	1
2. BACKGROUND	3
2.1 Bed and Suspended Load Concepts	4
2.2 Application of the Sediment Transport Model	6
3. THEORETICAL ANALYSIS	9
3.1 Model Development	9
3.1.1 Basic Assumptions	9
3.1.2 General Formulation	11
3.1.3 The Direct Einstein Method	13
3.1.4 Bed Profile Model	17
3.2 Results	19
4. EXPERIMENTAL WORK	26
4.1 Experimental Apparatus	26
4.1.1 Laboratory Reservoir	26
4.1.2 Sediment Feed	28
4.1.3 Sediment	30
4.1.4 Bedload Trap	30
4.1.5 Hot Film Annemometry	33
4.2 Experimental Procedures	34
4.3 Experimental Results	36
5. DISCUSSION OF RESULTS	40
6. SUMMARY AND CONCLUSIONS	47
REFERENCES	49

Page

APPENDICES

I	Direct Einstein Computer Package	50
II	Comparison of Computer Package Results to Einstein's	67
III	Bed Profile Computer Model	71
IV	Raw Data	76
	IV.1 Sediment Feed Rates	76
	IV.2 Bedload Trap Data	77
	IV.3 Velocity, Turbulence Intensity, and Depth Data	80
V	Velocity and Turbulence Intensity Relationships	106
VITA		109

LIST OF FIGURES

<u>Figure</u>	<u>Page</u>
2.1 $\Phi_* - \Psi_*$ Curve	8
3.1 Idealized Reservoir Sedimentation Scheme	10
3.2 Reservoir Approximated by Series of Uniform Flow Reaches	12
3.3 Ψ' vs. \bar{u}/u_*	16
3.4 Flow Chart for Bed Profile Model	20
3.5 Predicted Bed Profile	22
3.6 Predicted Variation of Bedload to Total Load Ratio with Distance	23
3.7 Predicted Bed Profile	24
3.8 Predicted Variation of Bedload to Total Load Ratio with Distance	25
4.1 Laboratory Reservoir	27
4.2 Sediment Feed Pipe	29
4.3 Sediment Grain Size Distribution	31
4.4 Section through Bedload Trap in Bed	32
4.5 Bedload Trap in Bed (slide)	32
5.1 Predicted and Measured Bed Profiles	41
5.2 Predicted and Measured Bed Profiles	42
5.3 Variation of Bedload to Total Load Ratio with Distance Theoretical Curve and Experimental Points	44
5.4 Variation of Bedload to Total Load Ratio with Distance Theoretical Curve and Experimental Points	45
AI.1 Correction Factor x	62
AI.2 Pressure Correction in the Transition to a Smooth Bed	63
AI.3 Hiding Factor	64
AV.1 Velocity and Turbulence Intensity; Flow Rate = 0.25 cfs	107
AV.2 Velocity and Turbulence Intensity; Flow Rate = 0.47 cfs	108

LIST OF TABLES

<u>Table</u>	<u>Page</u>
3.1 Sediment Size Fractions	19
4.1 Experimental Results: Run 1	38
4.2 Experimental Results: Run 2	39

1. INTRODUCTION

1.1 Introductory Remarks

Until recently, most research in the area of sediment transport has considered only steady, uniform flow conditions. However, there are many nonuniform flow situations in which the knowledge of sediment transport rates is important -- notably, the case of sedimentation in a reservoir. The rate and ultimate extent of sedimentation in a reservoir can be an important factor in the design and economic evaluation of a proposed impoundment.

The volume of sediment that will be deposited in a reservoir over a given period of time can easily be calculated if the average rate of sediment transport into the reservoir is known. This rate could be found by using any one of a number of uniform flow sediment transport models. However, the location of the deposited sediments, and the formation and growth of a delta, is not easily predicted.

A sediment transport model that includes nonuniform flow conditions could predict the development of sediment deposits and the ultimate steady state bottom profile in a reservoir. In practice, the steady state situation is perhaps more useful, and it is this problem that will be studied in this paper.

1.2 Scope of the Project

This report will consider a simple nonuniform flow situation, that of decelerating flow in a reservoir with diverging walls. The steady state sediment transport rates and deposition patterns for the flow scheme will be studied both analytically and experimentally.

Chapter 2 includes a brief discussion of background material, and outlines some of the basic concepts of Einstein's 1950 bedload function. Difficulties in adapting a uniform flow sediment transport model to a nonuniform flow are also discussed.

The analytical portion of the work is presented in Chapter 3. A technique for direct calculation of sediment transport rates from given flow conditions using Einstein's bedload function is developed. This is used to create a model that will predict transport rates in mildly non-uniform flows.

Chapter 4 describes the experimental work that was performed. Equipment and procedures that were used are detailed, and the results of the testing are presented.

The experimental results are compared to predictions obtained by applying the analytical model to the experimental flow conditions in Chapter 5. Difficulties encountered during the experimental work and in applying the model are also discussed.

Finally, conclusions will be drawn as to the validity of the model and limitations to its use.

2. BACKGROUND

The determination of sediment transport rates for the case of steady, uniform flow has received extensive treatment in the literature. For a reach of constant velocity, depth, and energy slope, the equilibrium transport rate for noncohesive sediment particles will be equal to the carrying capacity of the flow. If more sediment is introduced than the flow is able to carry, some must settle out and deposition will occur. If the carrying capacity of the flow is greater than the actual sediment transport rate, sediment will be eroded from the bed until the flow's carrying capacity is reached. The processes of erosion and deposition will, of course, affect the carrying capacity of the flow. In a uniform flow reach, therefore, a constant equilibrium sediment transport rate will be maintained.

For a general nonuniform flow situation, flow conditions -- and therefore sediment transport capacity -- will vary in both space and time. However, at a given point in space, the flow will gradually adjust to some set of equilibrium conditions through the process of erosion or deposition until the sediment transport rate is equal to the carrying capacity of the flow at that point. For the steady state situation that will occur after some period of time, the only variation of transport rates is spatial.

If the steady state nonuniform flow does not have abrupt variations in flow conditions -- that is, the flow is mildly nonuniform -- it can be approximated by a series of uniform flow reaches. The steady state nonuniform sediment transport problem has been simplified so that it can be analyzed using existing uniform flow sediment transport models.

2.1 Bed and Suspended Load Concepts

The total rate of sediment transport is equal to the sum of the bedload and suspended load transport rates. These transport rates are functions of sediment properties and flow conditions.

The suspended load consists of sediment particles that travel completely surrounded by the fluid flow, and are held in suspension by turbulent velocity fluctuations. The lower limit to the region of suspended load has been defined as several grain diameters from the bed, and at this boundary there is interaction and exchange between the bedload and suspended load.

If a logarithmic velocity distribution is assumed, it can be shown (1) that the concentration, C , of suspended sediment at depth y is:

$$C = C_a \left(\frac{D-y}{y} \frac{a}{D-a} \right)^z \quad (2.1)$$

$$z = \frac{v_{ss}}{k u_*} \quad (2.2)$$

where C_a is the reference concentration at a distance a from the bed. D is the total depth of flow, k is von Karman's constant, and u_* is the shear velocity. If a is taken as a few grain diameters, then C_a can be related to the bedload transport rate (2). The equation above can then be integrated over the depth of the region of suspension to determine the suspended load transport rate in terms of the bedload rate.

Bedload is understood to be the quantity of sediment particles moving in close proximity to the bed by rolling, sliding, and making short hops of a few grain diameters distance. One of the many models which have

been developed to predict bedload transport rates is Einstein's 1950 bedload function (2), which is based on statistical consideration of the forces on a particle.

Einstein's bedload function describes the relationship between two dimensionless parameters over a wide range of flow conditions. The intensity of bedload transport, Φ_* , is a function of the transport rate and the sediment properties. It is defined as

$$\Phi_* = k_1 \frac{g_s}{\gamma_s} \left[\frac{\rho}{\rho_s - \rho} \frac{1}{g d^3} \right]^{1/2} \quad (2.3)$$

k_1 = ratio of fraction of bedload to bed material of a given grain size

g_s = bedload transport rate

γ_s = specific weight of sediment

ρ = density of water

ρ_s = density of sediment

g = gravitational acceleration

d = sediment particle diameter

The flow intensity, Ψ_* , is a function of flow conditions and sediment properties:

$$\Psi_* = k_2 \frac{\rho_s - \rho}{\rho} \frac{d}{S_e R_b'} \quad (2.4)$$

where S_e is the energy slope of the flow and R_b' is the hydraulic radius with respect to the bed due to grain roughness. The factor k_2 includes the hiding factor for grains in a mixture, the change in lift coefficient for mixtures with various roughnesses, and the correction factor in the

logarithmic velocity distribution for the transition between hydraulically smooth and rough boundaries (2).

A statistical analysis, detailed by Einstein, (2), shows that the relationship between Φ_* and Ψ_* may be defined in terms of an error function:

$$\frac{A_* \Phi_*}{1 + A_* \Phi_*} = 1 - \frac{1}{\sqrt{\pi}} \int_{-B_* \Psi_* - 1/\eta_o}^{+B_* \Psi_* - 1/\eta_o} e^{-t^2} dt \quad (2.5)$$

$$\Phi_* = \frac{1}{A_*} \frac{P}{1-P} \quad (2.6)$$

$$P = 1 - \frac{1}{2} \left[\text{erf}(B_* \Psi_* + 1/\eta_o) + \text{erf}(B_* \Psi_* - 1/\eta_o) \right] \quad (2.7)$$

In the equations above, A_* , B_* , and η_o are universal constants which have been determined experimentally. A plot of Φ_* versus Ψ_* is shown in Figure 2.1.

Einstein's 1950 bedload function is considered to be one of the most theoretically complete bedload equations and will be used in this analysis.

2.2 Application of the Sediment Transport Model

Although Einstein's method has been accepted as a way to predict sediment transport rates, it proves to be cumbersome to use because the results are given in terms of sediment rating curves for a range of flow conditions. This is due to the procedure for calculations, which is detailed by Einstein in his 1950 paper (2).

For given channel cross section geometry, a series of values are assumed for the hydraulic radius with respect to the bed due to grain

roughness, R_b' . As the calculations progress, the hydraulic radius due to bedforms, R_b'' , can be found. The sum of these gives the total hydraulic radius with respect to the bed, R_b , which defines the flow rate. To find the sediment transport rate for a given set of flow conditions, interpolation between the calculated data is usually necessary. For this reason, Einstein's approach can be described as an indirect method for calculation of sediment transport rates.

For repetitive sediment transport calculations with various given flow conditions, however, it is desirable to be able to directly calculate the transport rates from the flow conditions, without interpolation. To do this using Einstein's method, it is necessary to find R_b' directly from R_b , as specified by the flow. A technique for doing this is described in Chapter 3, and is the basis for the Direct Einstein Method.

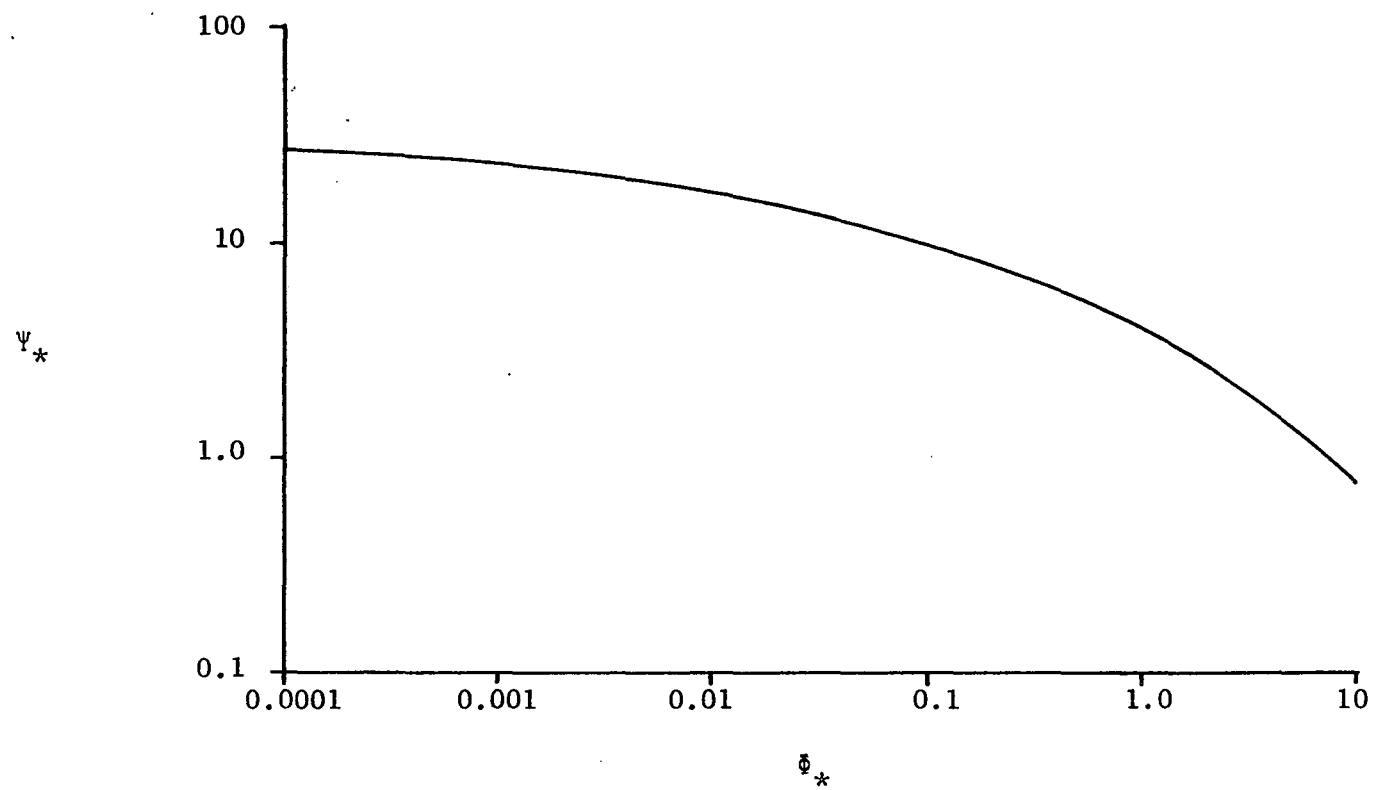


Figure 2.1 Φ_* - Ψ_* Curve (from Einstein, 1950)

3. THEORETICAL ANALYSIS

The theoretical analysis will be performed for a simple reservoir with straight, diverging walls and a constant flow rate. The problem to be solved will be confined to finding the steady state bed profile in the reservoir for a given constant inflow and incoming sediment transport rate. Einstein's 1950 method (2) for calculating sediment transport rates is modified to allow direct calculations. This technique is then used to develop a model to predict the steady state bed profile. The model is applied to conditions observed during experimental work to find the expected bed profile.

3.1 Model Development

3.1.1 Basic Assumptions

In order to predict the bed profile for the simple reservoir sedimentation situation shown in Figure 3.1, the following simplifying assumptions have been made.

1. Steady state conditions exist behind the advancing delta front.
The depth and velocity of flow at a point upstream from the delta front will remain constant. Small variations due to the motion of bedforms are not considered.
2. A mildly nonuniform flow region can be approximated by a series of small, uniform flow reaches.
3. A horizontal water surface profile exists in the reservoir; back-water effects are neglected.

The first two assumptions are necessary for the development of the model. The third is made primarily for convenience. Finding the effects

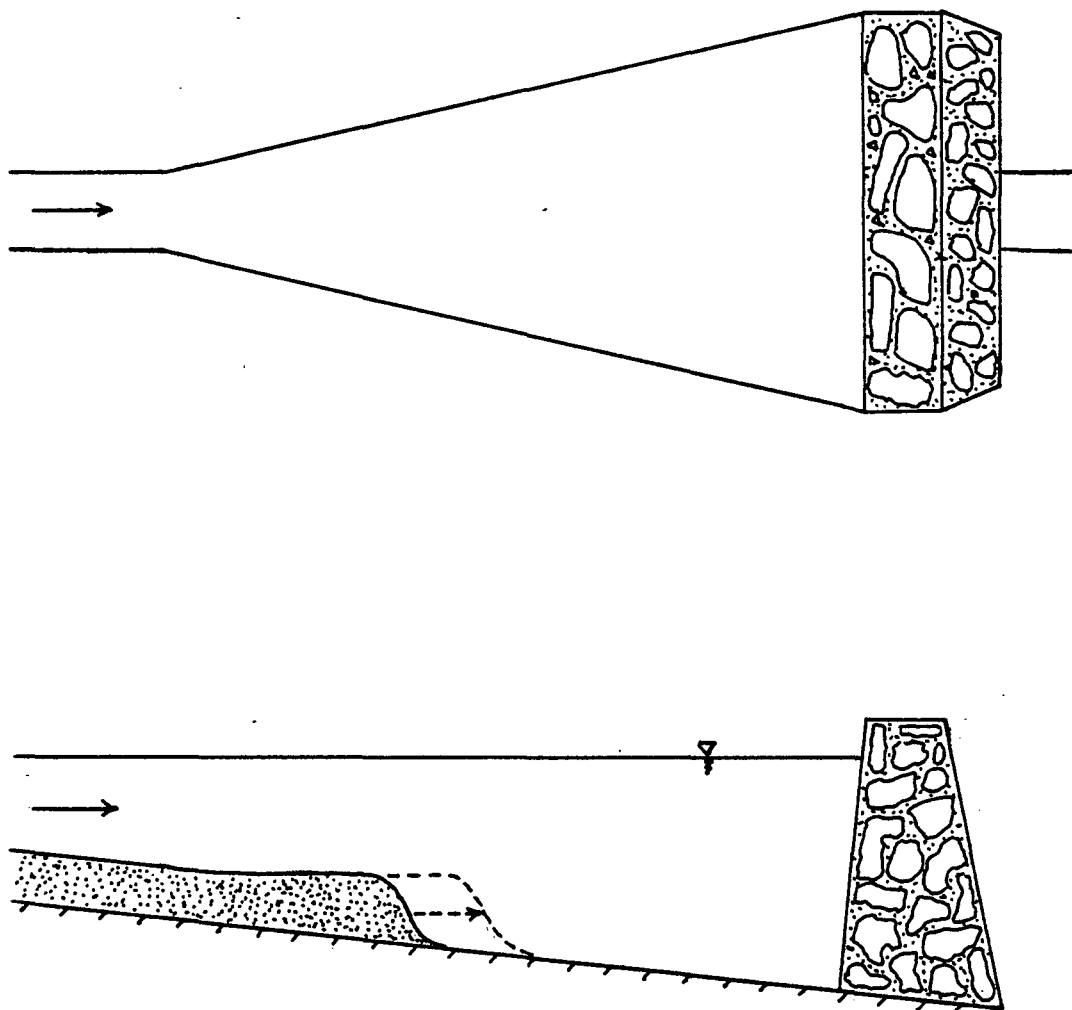


Figure 3.1 Idealized Reservoir Sedimentation Scheme

of a backwater profile would complicate the analysis to an extent that is beyond the scope of this report. Further discussion of the assumptions will be presented in a later section.

3.1.2 General Formulation

Since the simple reservoir shown in Figure 3.1 has no discontinuities or large nonuniformities, it can be approximated by a series of uniform flow reaches, as shown in Figure 3.2. Each uniform flow reach has a constant width, depth, velocity, and sediment transport rate at steady state conditions. It is assumed that the delta crest has progressed downstream from each flow reach considered, so that flow conditions are steady.

At steady state conditions, the total sediment transport rate into a reach will be equal to the total sediment transport rate out of the reach. Since the depth of flow remains constant, there is no net deposition or erosion within the reach. Although the sediment transport rate per unit width will vary from reach to reach as the width varies, the total transport rate must remain constant over the entire steady state region. The total transport rate through any cross section of the reservoir will be equal to the total rate of sediment transport into the reservoir.

It should be noted that for a given flow rate and channel cross section, the depth of flow is indicative of the magnitude of the rate of sediment transport. Increasing the depth will decrease the velocity of flow, and therefore the transport rate will decrease. Similarly, decreasing the depth will increase the sediment transport rate. It can be concluded that a specified total rate of sediment transport can exist at only one depth, for given channel geometry and flow rate.

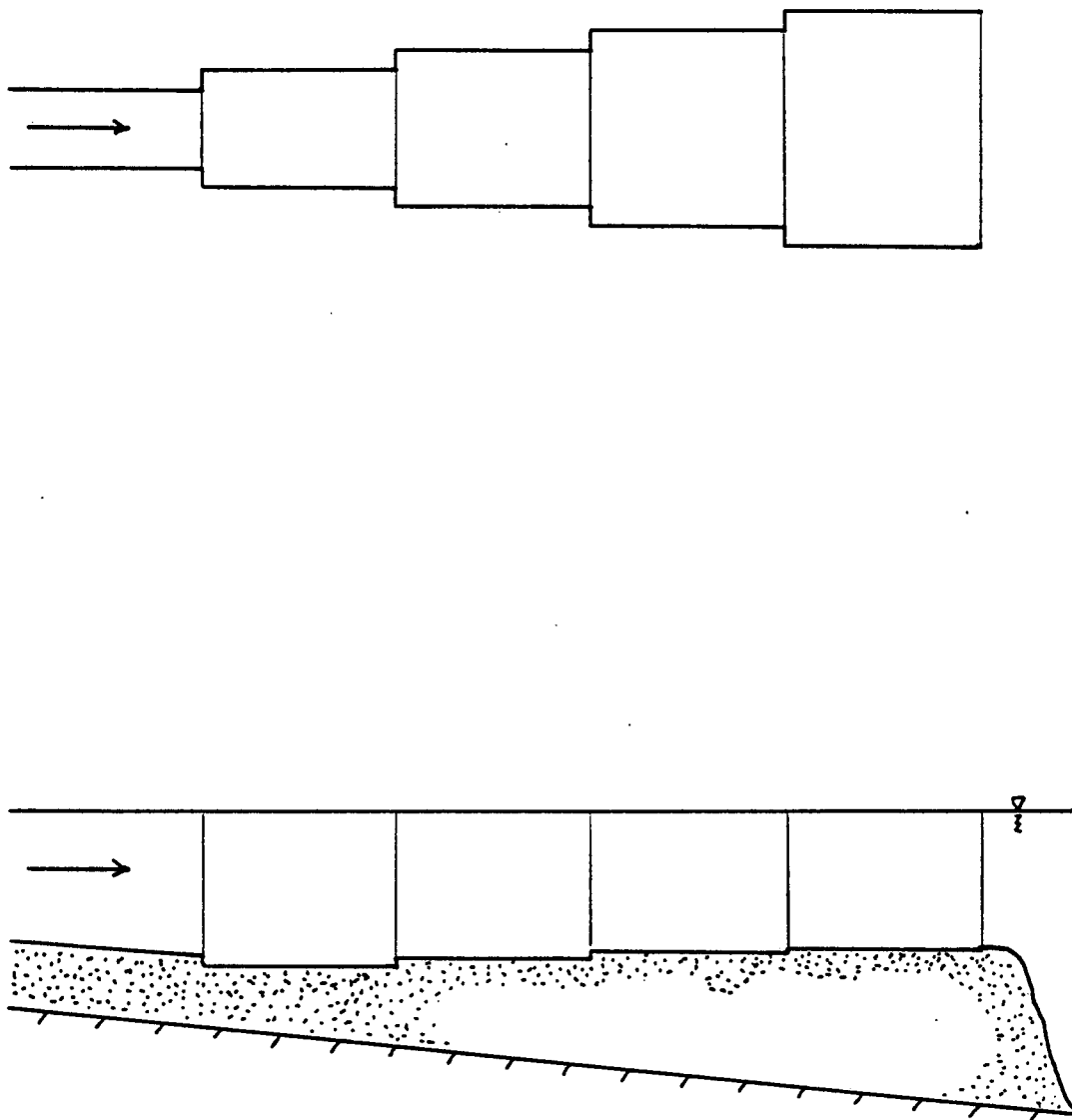


Figure 3.2 Reservoir Approximated by Series of Uniform Flow Reaches

The steady state bed profile of a reservoir can be found by calculating the depth corresponding to the total sediment transport rate into the reservoir for each of the uniform flow reaches that together approximate the diverging reservoir. Since the flow depth is involved in parameters such as velocity, hydraulic radius, and energy slope, the best approach to find the depth corresponding to a specific transport rate appears to be some kind of iterative procedure. It is advantageous, since several iterations may be required before the correct depth is found, to be able to directly calculate the sediment transport rate for the assumed depth and corresponding flow conditions. This is not possible using Einstein's method as described in his 1950 paper. Therefore, a more direct calculation technique has been devised and is outlined in the next section.

3.1.3 The Direct Einstein Method

The calculation procedure outlined by Einstein (2) results in a sediment discharge rating curve for a particular channel cross section and energy slope. The method is useful if the sediment transport rates over a range of flow conditions are desired. However, it is time consuming to construct a rating curve if the transport rate for only one flow is needed. Einstein's equations can be used to directly calculate the transport rate for a specified set of flow conditions if a modification of his procedure is used.

One of the important parameters in Einstein's 1950 bedload function is the hydraulic radius with respect to the bed due to grain roughness, R_b' . This and the hydraulic radius with respect to the bed due to the bedforms, R_b'' , are added to give the total hydraulic radius with respect

to the bed. These two components of the hydraulic radius must be separated before sediment rate calculations can proceed.

According to Keulegan (6), the average velocity for the entire transition between a hydraulically smooth and rough bed may be related to the hydraulic radius due to grain roughness by the following equation:

$$\bar{u} = u_*' 5.75 \log_{10} \left(12.27 \frac{R_b' x}{k_s} \right) \quad (3.1)$$

\bar{u} = average flow velocity

$u_*' = \sqrt{g R_b' S_e}$, the shear velocity due to grain roughness

x = a correction factor for the transition from a hydraulically smooth to rough bed.

k_s = the roughness diameter of the bed expressed as a representative grain diameter, usually taken as D_{65} .

A similar expression may be written relating the average velocity to R_b'' , and would be expected to be a function of the bedforms. The bedform patterns vary with the sediment transport rate, and therefore the flow conditions. Einstein has expressed the quantity \bar{u}/u_*'' as a function of the flow parameter, Ψ' .

$$\Psi' = \frac{\rho_s - \rho}{\rho} \frac{D_{35}}{R_b' S_e} \quad (3.2)$$

Using the relationship between \bar{u}/u_*'' and Ψ' shown in Figure 3.3, Einstein's procedure for separating the two components of the hydraulic radius and defining the flow conditions is as follows:

1. Assume a value for R_b'
2. Obtain the correction factor for the velocity distribution
 $x = f(D_{65}, \text{thickness of the laminar sublayer})$

3. Calculate the average velocity using Equation 3.1
4. Calculate Ψ' using Equation 3.2
5. Find \bar{u}/u_*'' from Figure 3.3, and compute u_*''
6. $R_b'' = (u_*'')^2 / (g S_e)$
7. The total hydraulic radius with respect to the bed, R_b , is the sum of R_b' and R_b''
8. From the channel geometry and R_b , the area of flow can be found
9. The flow rate for the value of R_b' assumed is the product of the area and the average velocity.

Aside from the fact that this procedure makes it difficult to find R_b' and R_b'' for a specific flow rate, it has been discussed in the literature (1,3) that there is a substantial amount of scatter in the data used to construct the curve defining the relationship between \bar{u}/u_*'' and Ψ' . At high and low values of Ψ' , the points systematically depart from the curve shown in Figure 3.3. In fact, laboratory flume data were found to fall along a different curve than field data (4). The use of a relationship between \bar{u}/u_*'' and Ψ' to find the hydraulic radius component due to bed-forms may introduce errors into the calculations.

In order to directly calculate the sediment discharge rates for a flow with known velocity, total hydraulic radius, and energy slope, it is only necessary to find R_b' corresponding to the flow conditions before the sediment calculations can proceed. Examination of Equation 3.1 shows that all of the variables on the right hand side are known or can be expressed in terms of R_b' . It is possible to find R_b' corresponding to the known flow velocity without the knowledge of the specific relation between \bar{u}/u_*'' and

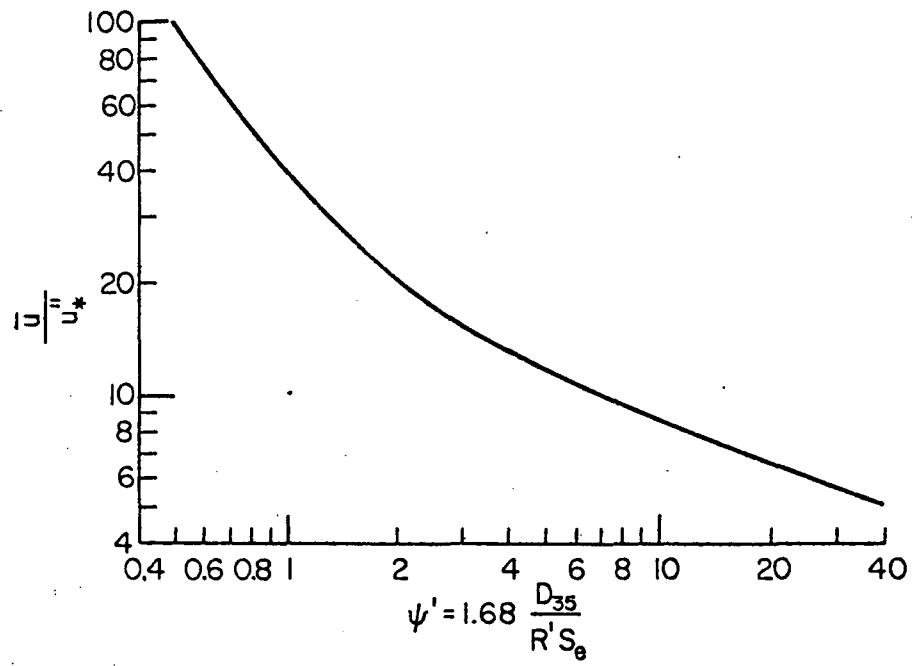


Figure 3.3 ψ' vs. \bar{u}/u''_* (from Einstein, 1950)

Ψ' . Once R_b' is known, it is a relatively simple matter to follow the rest of Einstein's procedure to calculate the sediment discharge rate.

A computer program has been written to evaluate Einstein's bedload function directly from given flow conditions. The following bisection iterative technique is used to find the appropriate R_b' for the flow.

1. Assume R_b' , noting that $0 \leq R_b' \leq R_b$
2. Find correction factor x for the velocity distribution
 $x = f(D_{65}, \text{thickness of the laminar sublayer})$
3. Calculate the average velocity using Equation 3.1
4. If the calculated velocity does not agree with the actual velocity, adjust R_b' :
 - a. If the calculated velocity is too large, the assumed R_b' is too large
 - b. If the calculated velocity is too small, the assumed R_b' is too small
5. Continue iteration until the calculated velocity is sufficiently close to the actual velocity.

The computer package has been shown to produce results nearly identical to those found by Einstein (2), and is a fast direct method for calculating sediment transport rates. See Appendix II for a comparison of results from the two procedures. The details and documentation for the computer program are found in Appendix I.

3.1.4 Bed Profile Model

The previously described package of computer subroutines provides an easy method for calculating the sediment transport rate corresponding

to a given depth, velocity, and energy slope. A driving program has been written to evaluate the steady state bed profile for a reservoir with straight diverging walls.

Use of the model requires that the total sediment transport rate into the reservoir be known for the flow rate of interest. Other input parameters include the reservoir geometry, Manning's roughness coefficients for the total flow and for the walls of the reservoir, and the sediment properties. The sediment properties required are the specific gravity, D_{35} , D_{65} , and particle diameters and size fractions. It is assumed that the reservoir can be approximated by a series of uniform flow reaches, as shown in Figure 3.2, and that a horizontal water surface profile exists.

An iterative procedure is used to find the depth corresponding to the total load transport rate (which is constant at all points in the reservoir for steady state conditions) for each of the uniform flow reaches. Since mean values of the hydraulic parameters over each reach are used in the computations, the length chosen for the reaches influences the accuracy of the results. For a reach of known width, a depth is assumed and the velocity and hydraulic radius corresponding to the flow are computed. The energy slope is found using Manning's equation, and the hydraulic radius with respect to the bed is separated from the overall hydraulic radius as suggested by Einstein (2). The sediment transport rates per unit width for each sediment size are then computed, and these are summed and multiplied by the reservoir width to get the total load transport rate for the assumed depth. If the calculated rate is not sufficiently close to the steady state transport rate, the depth is adjusted accordingly and a new iteration begins.

A flow chart for the bed profile model is shown in Figure 3.4, and the Fortran listing for the program is contained in Appendix III.

3.2 Results

The bed profile computer model was used to predict the steady state bed profile for the laboratory reservoir used in the experimental work, as described in Chapter 4. The flow and total sediment transport rates specified for the program were those actually measured during the experimental work. The computer program output was used to construct plots of the theoretical bed profile, and also the theoretical variation of the bedload transport rate as a percentage of the total load with distance into the reservoir.

The linear variation of width for the reservoir was 0.0917 feet per foot, so that the flow was mildly nonuniform. A Manning roughness coefficient of 0.013 was chosen for both the total flow and the walls of the reservoir. Five sediment size fractions for the sand described in section 4.1.3 were chosen, and are tabulated in Table 3.1.

Table 3.1 Sediment Size Fractions

Particle Diameter	Fraction of Bed Material
0.000243 ft	0.193
0.000410	0.195
0.000531	0.213
0.000689	0.356
0.001060	0.053

Two sets of measured flow and total sediment inflow rates were specified for the program. The theoretical bed profile for a flow rate of 0.25 cubic feet per second and a total sediment inflow rate of 0.00572

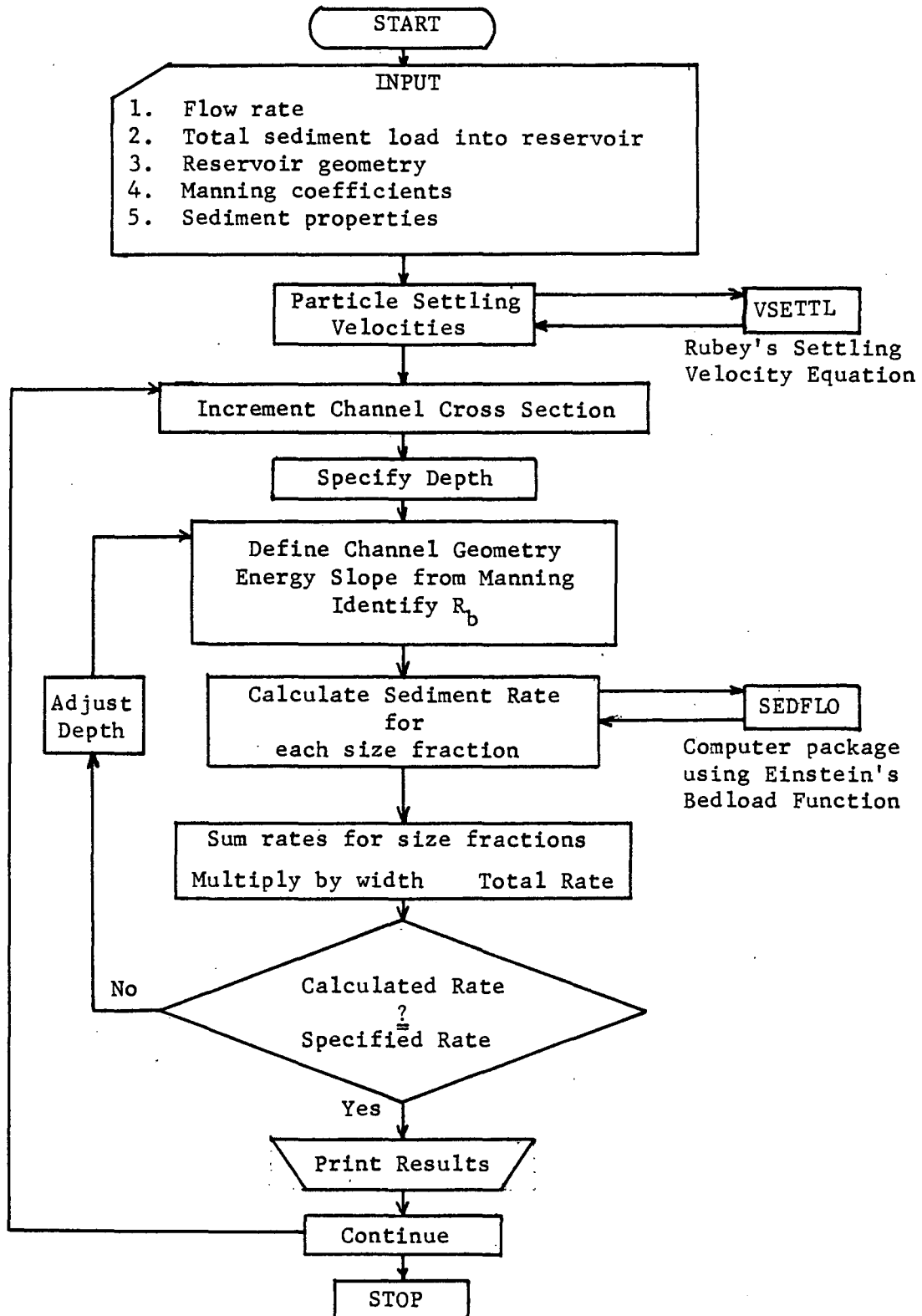


Figure 3.4 Flow Chart for Bed Profile Model

pounds per second is shown in Figure 3.5. The theoretical variation of the bedload fraction for these rates is shown in Figure 3.6. The corresponding plots for a flow rate of 0.47 cubic feet per second and a total sediment transport rate of 0.0499 pounds per second are shown in Figures 3.7 and 3.8. Further discussion of the bed profile model and comparison of the bed profile model and comparison with experimental results is contained in Chapter 5.

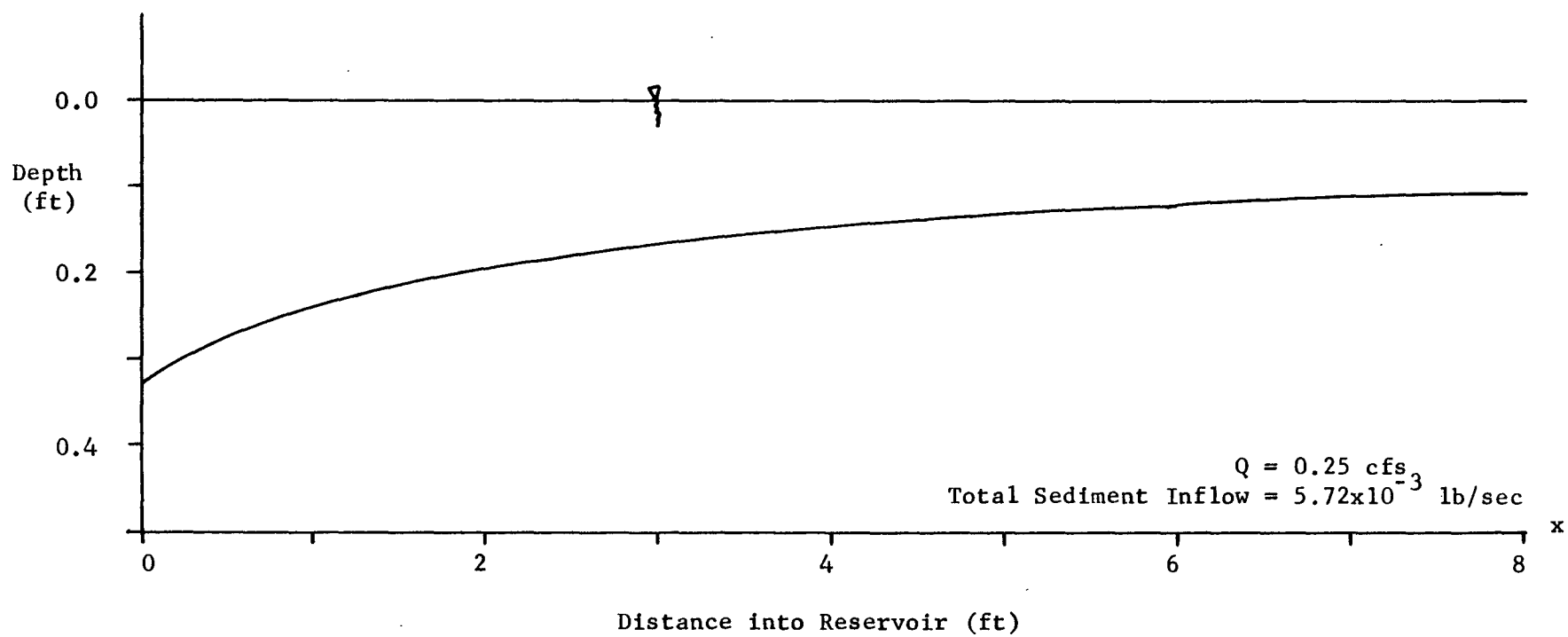


Figure 3.5 Predicted Bed Profile

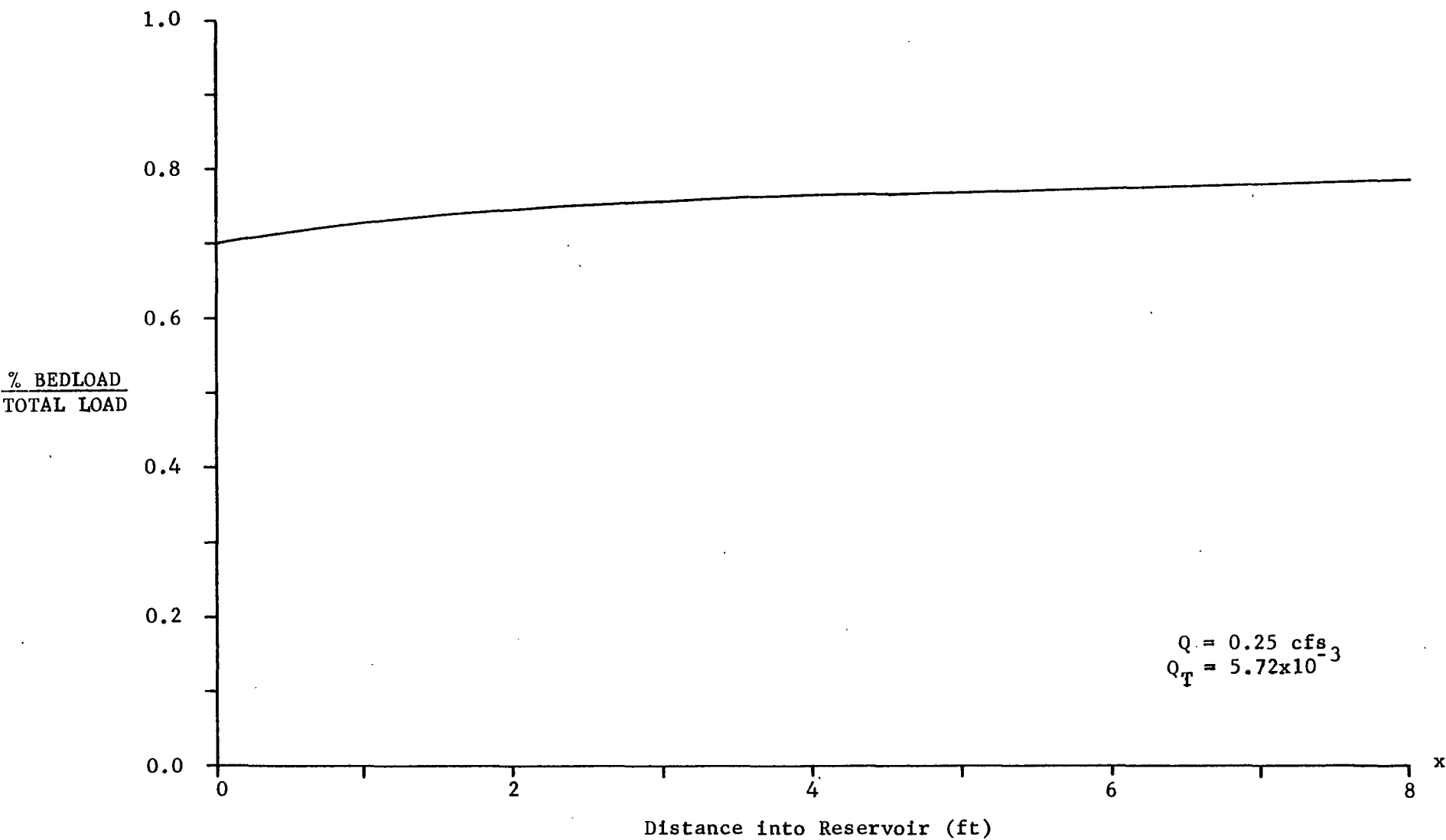


Figure 3.6 Predicted Variation of Bedload to Total Load Ratio with Distance

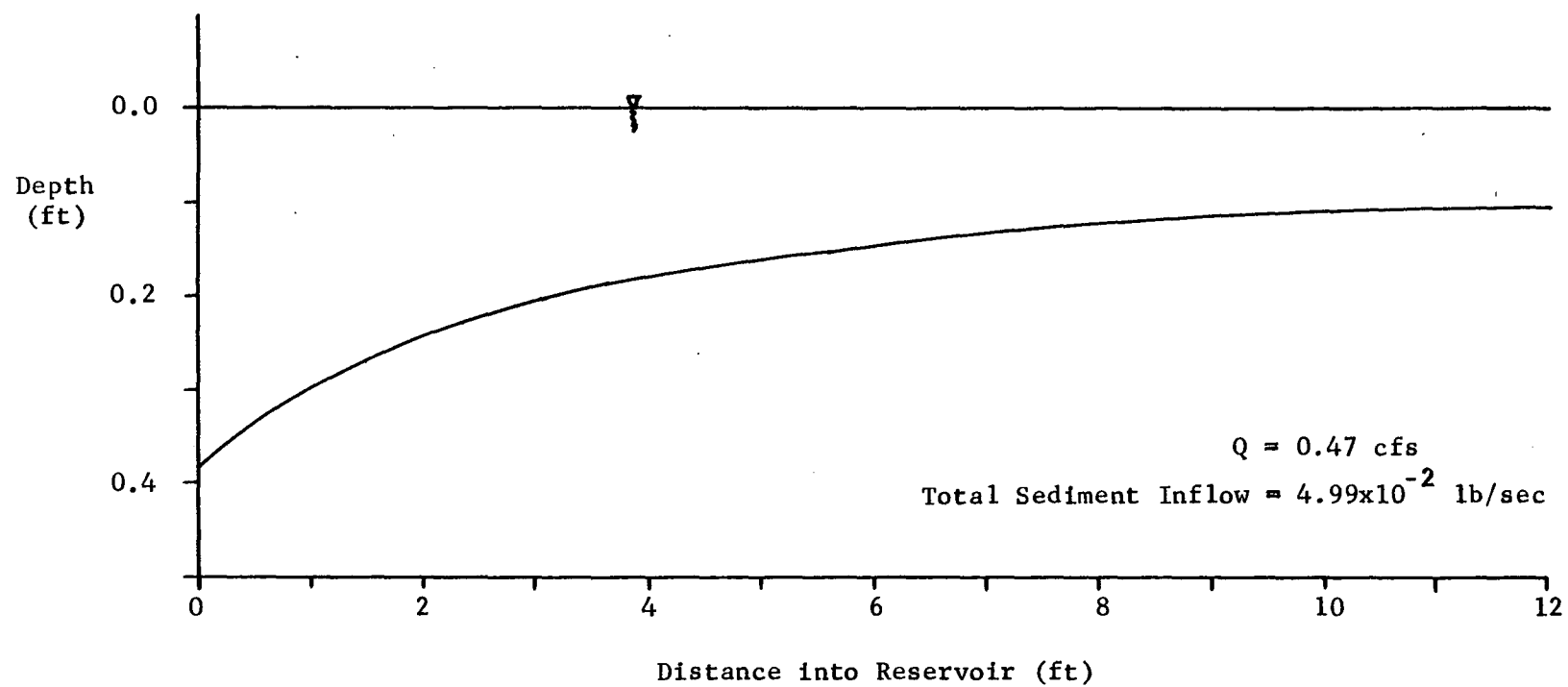


Figure 3.7 Predicted Bed Profile

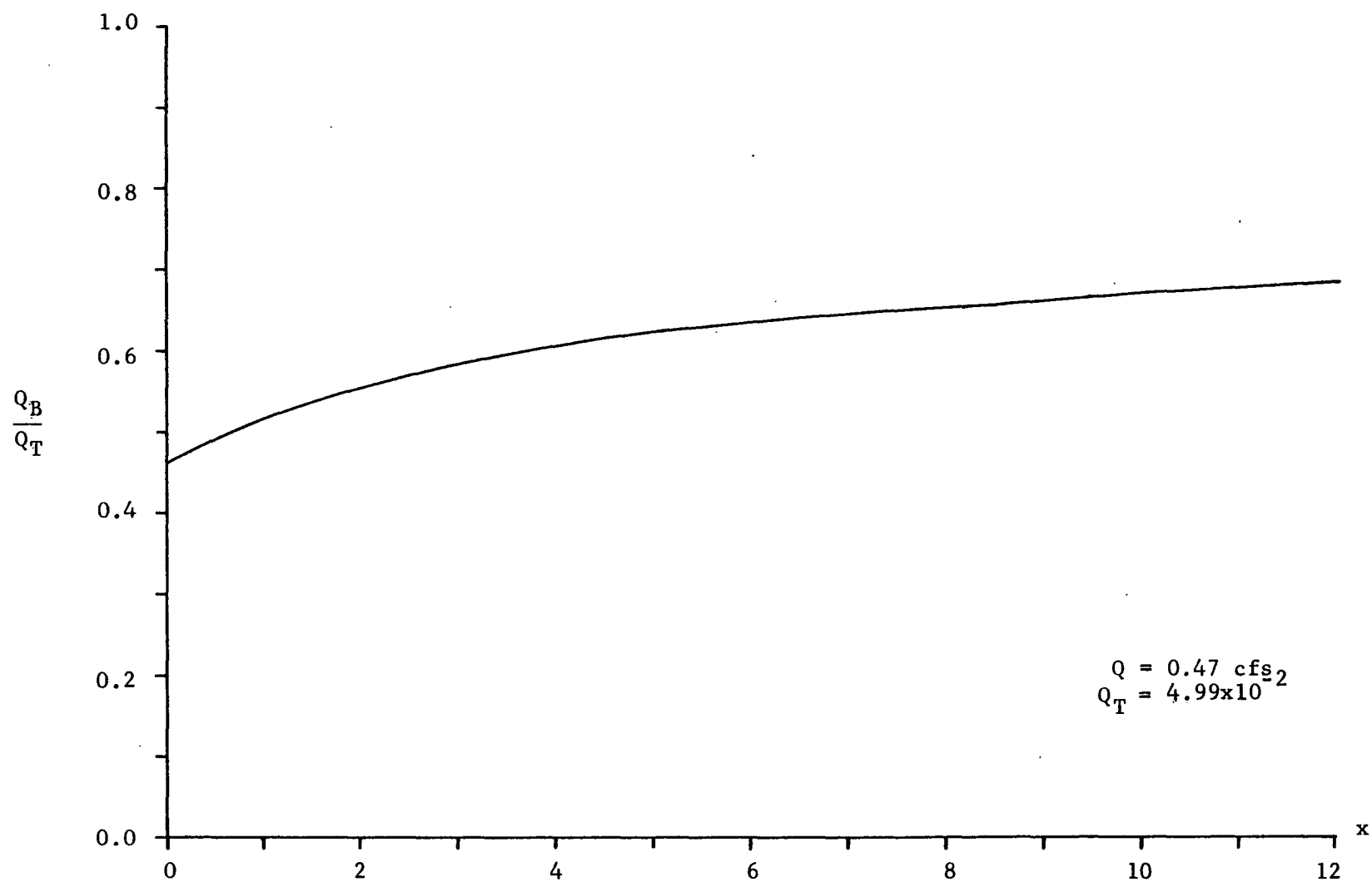


Figure 3.8 Predicted Variation of Bedload to
Total Load Ratio with Distance

4. EXPERIMENTAL WORK

In order to investigate the validity of the analytical bed profile model presented in Chapter 3, a laboratory reservoir was constructed. Sediment was fed into the reservoir at a measured rate, and the steady state bed profile that developed was recorded, as well as the bedload transport rates through various cross sections in the steady state region. The equipment and procedures used and the results obtained from the experimental work are presented in this chapter.

4.1 Experimental Apparatus

4.1.1 Laboratory Reservoir

The laboratory reservoir used for the experimental work is shown in Figure 4.1. It consisted of a short, 6 inch wide straight approach channel entering a reservoir section that diverged to an ultimate width of five feet. The reservoir was not symmetrical with respect to the approach channel, as it was constructed using the steel wall of a large flume as a continuous wall for one side of the approach channel and the reservoir. The other wall was made of plywood, and had plexiglass windows located at intervals along it so that the bed profile could be readily observed.

The approach channel and the initial 8 feet of the reservoir had a horizontal bottom, while the rest of the reservoir had a bottom slope of 0.037 feet per foot (see Figure 4.1). Most of the measurements were performed in the first 8 feet of the reservoir, and the horizontal bottom there reduced the amount of sediment needed to achieve steady state conditions.

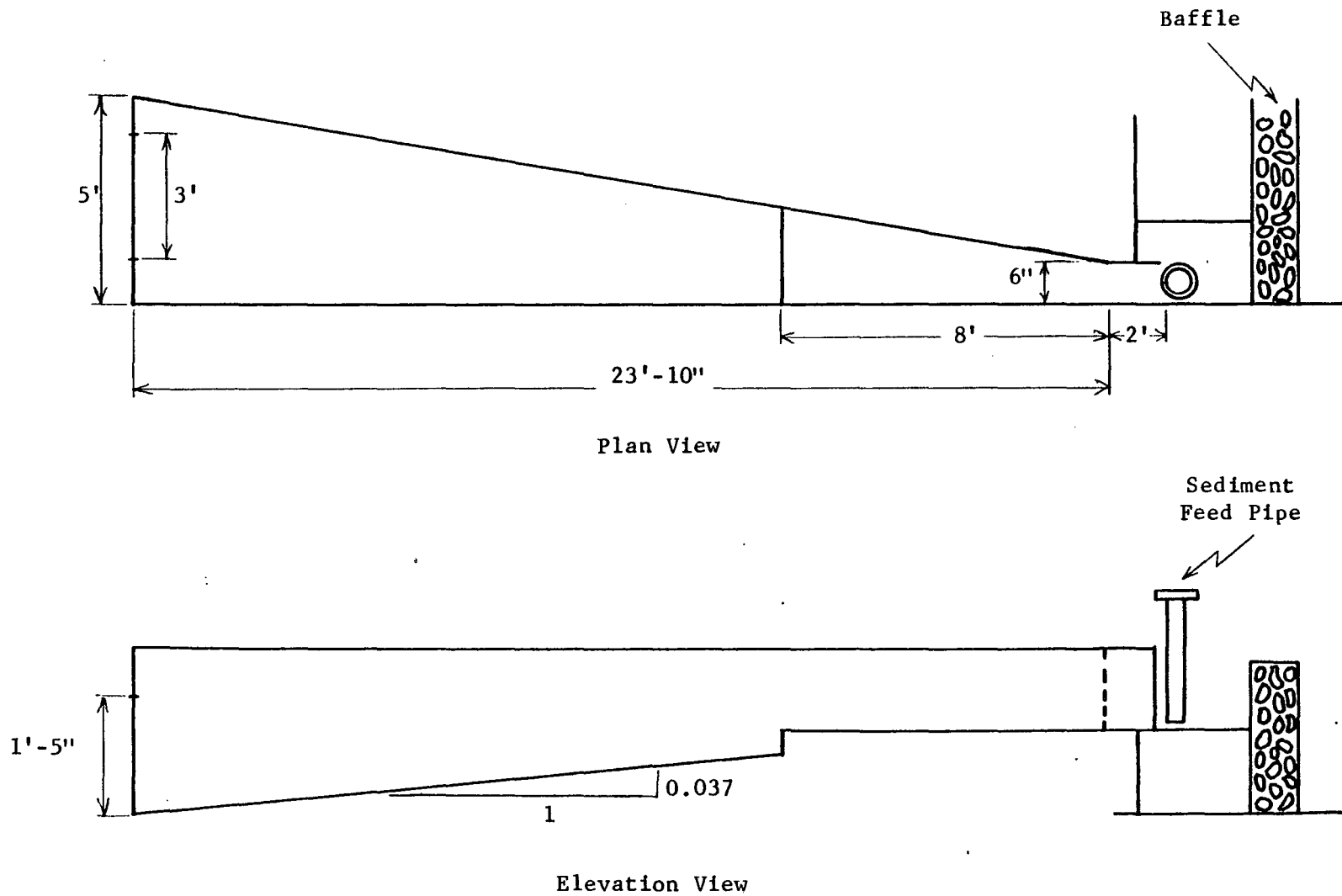


Figure 4.1. Laboratory Reservoir

Water entered the approach channel to the reservoir from a baffled head box. The flow rate into the head box was controlled by a valve on the water supply line. Water exited the reservoir over a 3 foot wide rectangular weir, and was returned to a sump for recirculation. The flow rate through the reservoir was measured with a hot film anemometry unit, as described in Section 4.1.5.

4.1.2 Sediment Feed

After several trial runs, it was determined that the best way to introduce sediment to the approach channel was through a vertical 4 inch diameter pipe that was raised approximately $3/4$ inch off the channel bottom, as shown in Figure 4.2. The sand feed pipe was located just upstream of the 6 inch wide approach channel (see Figure 4.1).

The feed pipe was filled with sand, which flowed out the bottom of the pipe and was carried away by the water flowing into the approach channel. Water was introduced at the top of the feed pipe to reduce the chance of clogging, and more sand was added to the pipe as required.

The equilibrium sand feed rate was dependent on the flow of water in the approach channel. As sediment was removed from the approach channel and was carried into the reservoir, it was replaced by sand carried away from the bottom of the feed pipe. The total sediment transport rate into the reservoir was determined by measuring the dry weight of sand fed into the sediment feed pipe over a period of time. It was observed during experimentation that the sand feed was fairly uniform, and that a

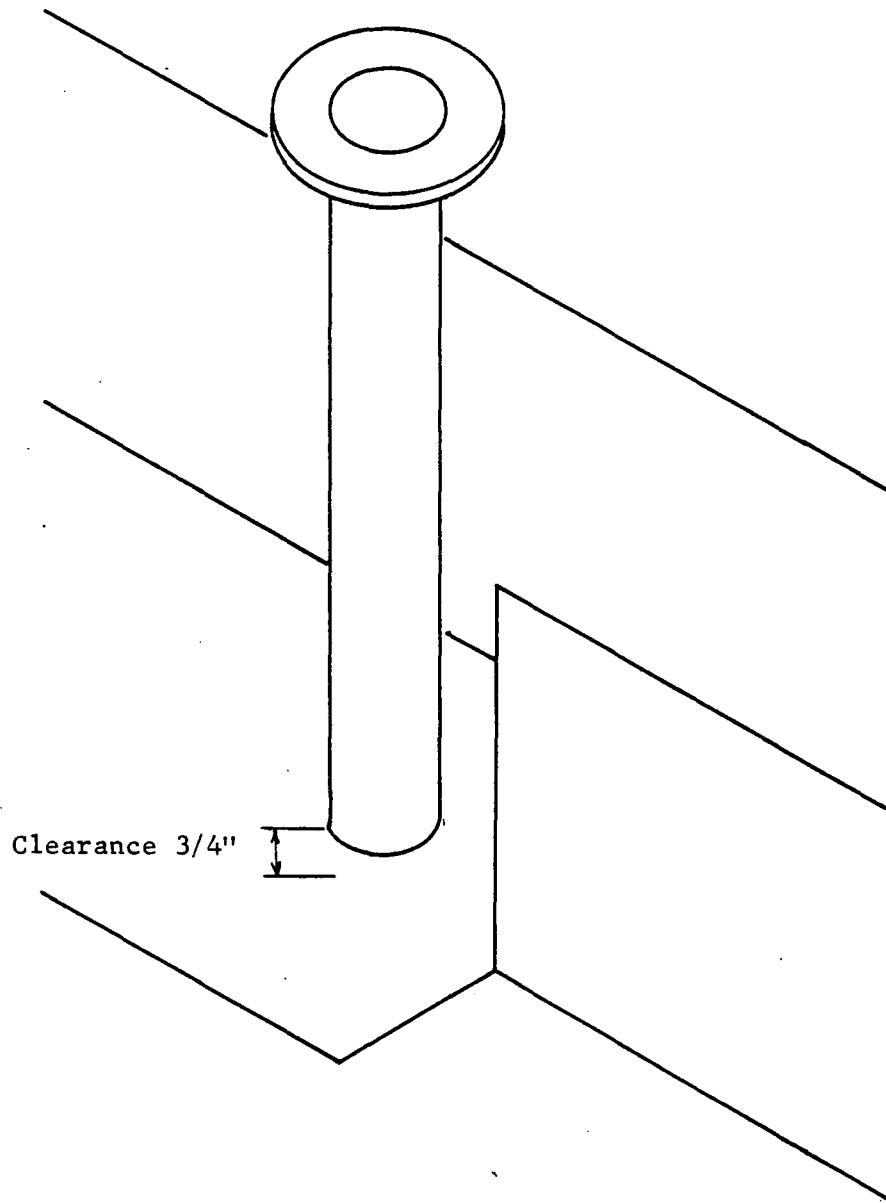


Figure 4.2 Sediment Feed Pipe

relatively constant sediment inflow to the reservoir could be maintained if the flow rate of the water entering the approach channel was constant. Disturbances to the flow caused by the feed pipe were minimal at the downstream end of the approach channel.

4.1.3 Sediment

The sediment used in the experimentation was a foundry sand with a specific gravity of 3.25 and a median grain diameter of 0.16 millimeters. A grain size distribution curve for the sand is shown in Figure 4.3. The sand was particularly well suited for the experimental work performed because it was fine enough to be easily suspended by the low flow rates required by the apparatus, so that some fraction of the total sediment transport rate was suspended load. Trial runs with coarser sands showed that the mode of transport was predominantly bedload. Use of the fine foundry sand made it possible to determine the variation of bedload as a fraction of the total load with distance into the reservoir.

4.1.4 Bedload Trap

The rate of bedload transport through a particular cross section of the reservoir was measured with a 2 inch by 2 inch by 12 inch sheet metal box that was buried in the center of the bed. This bedload trap was placed in the bed with its top edges slightly below the elevation of the bed and bedload material entered and was collected as it was carried along with the flow. The sides of the box that were parallel to the direction of flow were approximately 2 inches higher than the other two sides of the trap in order to prevent the entry of material from directions other than parallel to the flow. Figures 4.4 and 4.5 show the bedload trap placed in the bed.

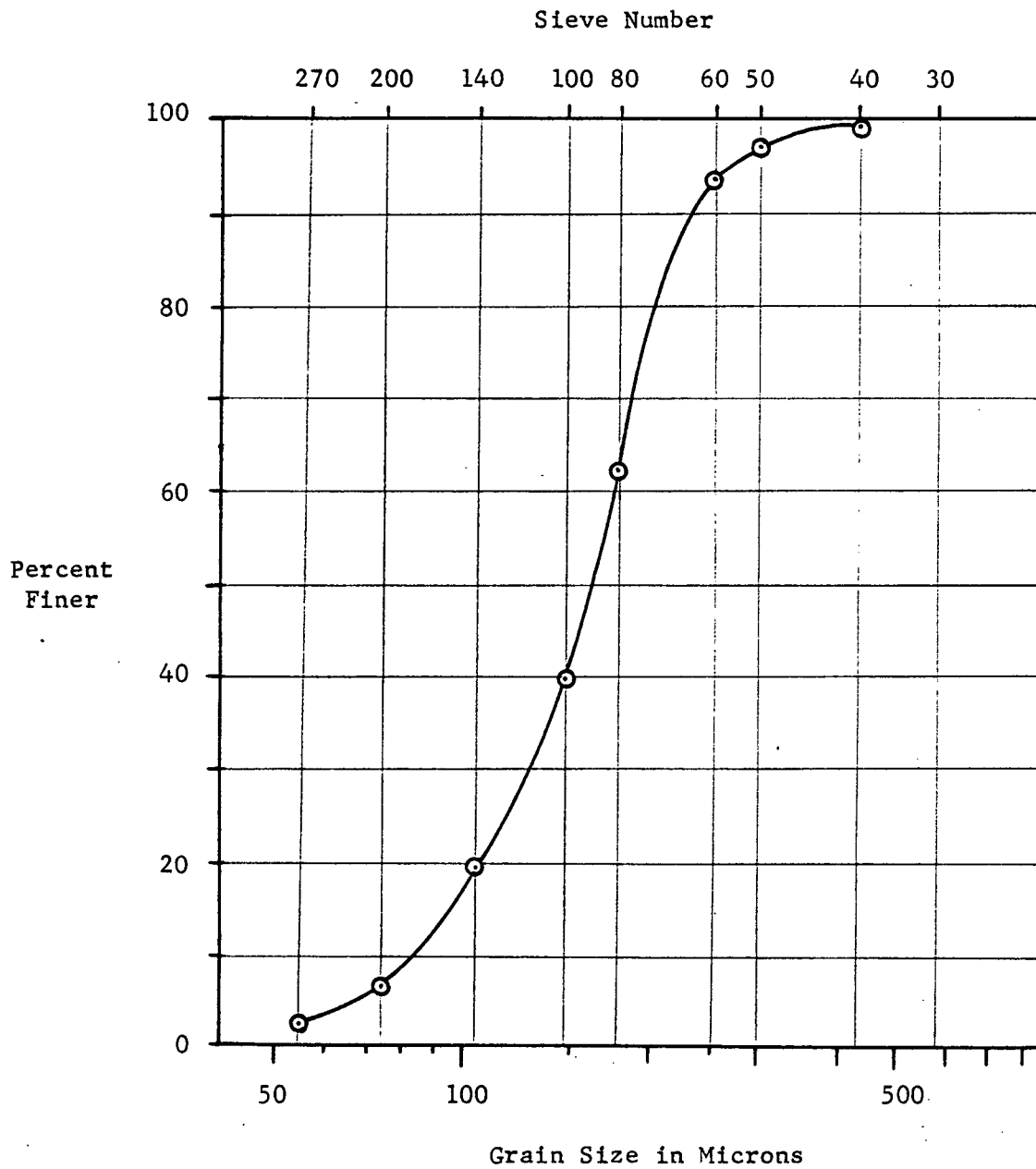


Figure 4.3 Sediment Grain Size Distribution

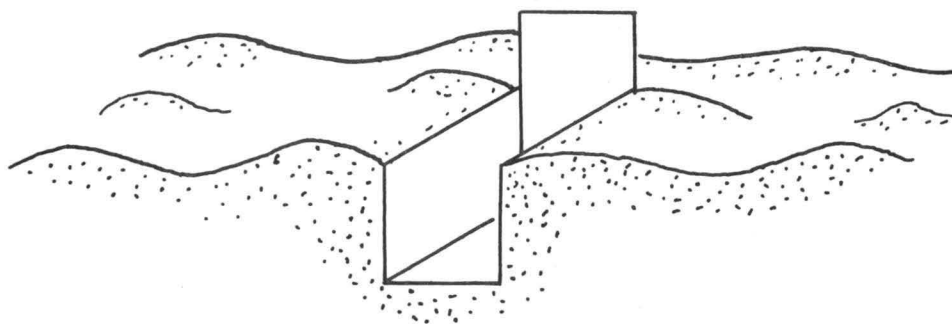


Figure 4.4 Section through Bedload Trap in Bed



Figure 4.5 Bedload Trap in Bed

It was realized that bedload measurement using a device of this type would not be entirely accurate, yet it was expected that the measurements obtained would give a good indication of the magnitude of bedload transport. Some practice was necessary to position the trap in the bed so that flow disturbances and scour around the trap were minimized, particularly if bedforms were present.

After the bedload trap was placed in the bed, sediment was allowed to flow into and around the trap until any disturbances caused by the placement of the trap were eliminated. Any sand in the trap was removed by hand, and the trap was allowed to fill for a measured period of time. The bedload trap was removed from the flow and emptied before it filled to the point that material deposited in the trap was caught by the flow and carried away as bedload again. The trap appeared to perform well, and it was assumed that the average bedload rate obtained from several measurements was representative of the true bedload transport rate.

4.1.5 Hot Film Annemometry

The flow velocity at each reservoir cross section considered during the experimental work was determined through measurements made with a DISA Type 55R42 conical hot film probe and a DISA Type 55D01 annemometer unit, along with digital and RMS voltmeters. The turbulence intensity of the flow was also recorded at each point where the velocity was measured. The equipment was calibrated by towing the probe in still water for velocities up to 3 feet per second, and was operated as directed in the user's manual.

The hot film probe was mounted at the bottom of a point gage that was attached to a moveable bridge, and could be positioned anywhere in the reservoir. At each reservoir cross section where measurements were taken, velocity data was recorded for several depths on verticals spaced every 2 inches across the width. The point gage was used to record the flow depth at each vertical. The velocity and depth data for each cross section were later reduced and used to calculate the average depth and flow rate at the section.

4.2 Experimental Procedures

The experience gained during the construction of the apparatus and during several trial runs was used to develop a systematic procedure for collecting data in the idealized laboratory reservoir. The procedure was followed as closely as possible in order to insure that all the data was taken under similar conditions.

Two hydraulic flow rates were studied in the laboratory, which resulted in two different total sediment transport rates into the reservoir. The higher flow rate produced a predominantly plane bed on the delta formation, with small bedforms developing near the delta crest. The lower flow produced well developed bedforms over the entire length of the delta, which meant that taking data was more difficult. The low flow rate was the first for which data was taken.

After the desired flow rate through the reservoir (which contained no sediment initially) was established, the water surface elevation immediately upstream from the overflow weir was established using a point gage that was permanently mounted there. This was used as a reference to

reestablish the same flow rate if the pump was stopped between sets of measurements. Although the flow rate for each run was determined precisely with the hot film annemometry unit, the water surface elevation at the weir was used to get an approximate value for the flow rate.

Sand was placed in the feed pipe and was carried into the reservoir, which eventually created a delta. The delta was allowed to progress until its crest was 8 feet into the reservoir before any data was taken. This insured that steady state conditions were present over at least the first 8 feet of the reservoir. As data was taken over that section, the delta continued to grow, allowing measurements to progress downstream.

Velocity, depth, and turbulence intensity data were taken for cross sections spaced at $\frac{1}{2}$ or 1 foot intervals into the reservoir. Using the hot film annemometry unit with the probe mounted on a point gage, measurements were taken at vertical sections spaced every two inches across the width of the reservoir. Several measurements were taken at each vertical section along with the water surface and bottom elevations. The data were later reduced to obtain average values for velocity, depth, and turbulence intensity at each cross section.

The total sediment transport rate into the reservoir was determined by measuring the dry weight of sand that was fed through the feed pipe over a period of time. This was done at the same time that the bedload trap was used to measure the bedload transport rate at a cross section. The sediment feed rates obtained were averaged to determine a representative total sediment transport rate into the reservoir.

The bedload transport rate through a reservoir cross section was found by placing the bedload trap in the bed and allowing particles to

deposit over a measured time. The trap was carefully placed in the bed to minimize scour and other disturbances. Any sand caught in the trap during placement was removed, and then timing for the measurement began. When the trap was between 1/3 and 1/2 full, it was removed from the flow and the accumulated sediment removed for drying and weighing. At least five measurements were taken for each cross section, since the instantaneous bedload rate varied depending on the bedforms present. Bedload rates were visibly greater when a bedform approached the trap than when the trap was between bedforms. By averaging the results of five measurements, a representative bedload rate was determined.

For the first flow rate, velocity and depth data were taken at $\frac{1}{2}$ -foot intervals and bedload data at 2-foot intervals for eight feet into the reservoir. At this distance, the bedforms became large enough compared to the depth of flow so that reliable data could not be taken. The reservoir was drained and the sand removed, and then the second (higher) flow rate was established. Data was taken following the same procedures, this time extending for 11 feet into the reservoir, where bedforms again prevented taking accurate data. No bedforms were present in the first 7 or 8 feet of the reservoir, so reliable data could be obtained by taking velocity and depth data at one foot intervals. Bedload rates were again measured at 2 foot intervals down the reservoir.

4.3 Experimental Results

Results from the experimental investigation of sediment transport in the laboratory reservoir are contained in Tables 4.1 and 4.2. The raw and reduced data from which these results were derived appear in Appendix IV. The first flow rate investigated was 0.25 cubic feet per second and

produced a total sediment transport rate into the reservoir of 0.00572 pounds per second. The second experimental run was at an average flow rate of 0.47 cfs with a total transport rate of 0.0499 lb/sec.

The tables show the values of the depth, velocity, and bedload transport rates that were measured in the laboratory. Appendix V contains a summary of the velocity and turbulence intensity trends that were observed. Discussion of the experimental results and comparison to the analytical predictions are contained in Chapter 5.

Table 4.1 Experimental Results: Run 1

Average Flow Rate: 0.25 cfs

Average Total Sediment Transport Rate: 0.00472 lb/sec

Distance into Reservoir (ft)	Depth (ft)	Velocity (ft/sec)	Bedload Transport Rate (lb/sec/ft)
0.0	0.357	1.41	
1.0	0.296	1.38	0.00431
1.5	0.253	1.14	
2.0	0.203	1.10	
2.5	0.170	1.23	
3.0	0.189	1.18	0.00210
3.5	0.180	1.07	
4.0	0.160	1.00	
4.5	0.162	1.18	
5.0	0.159	1.30	0.00174
5.5	0.148	1.34	
6.0	0.138	1.25	
6.5	0.143	1.06	
7.0	0.142	1.22	0.00205
7.5	0.103	1.15	
8.0	0.106	1.16	

Table 4.2 Experimental Results: Run 2

Average Flow Rate: 0.47 cfs

Average Total Sediment Transport Rate: 0.0499 lb/sec

Distance into Reservoir (ft)	Depth (ft)	Velocity (ft/sec)	Bedload Transport Rate (lb/sec/ft)
2.0	0.185	2.64	
3.0	0.170	2.61	0.0281
4.0	0.138	2.90	
5.0	0.114	2.79	0.0261
6.0	0.104	2.70	
7.0	0.091	2.65	0.0260
8.0	0.101	2.47	
9.0	0.086	2.33	0.0181
10.0	0.093	1.90	
11.0	0.101	1.90	0.0124

5. DISCUSSION OF RESULTS

The analytical bed profile model based on the approximation of a nonuniform flow region by a series of uniform flow reaches was used to predict the bed profile for the laboratory reservoir, as discussed in Chapter 3. The comparisons of the predictions and the experimental measurements for the bed profiles at flow rates of 0.25 cubic feet per second and 0.47 cfs are depicted in Figures 5.1 and 5.2.

Although there is some scatter in the experimental points, the trend is obvious. The scatter is due in part to the difficulties in obtaining an average depth value for a changing bed with moving bedforms. It should be noted that the variation of the experimental points is never more than a few hundredths of a foot.

The analytical predictions follow the trend of the data points quite well. It is interesting to note that the prediction for the flow of 0.25 cfs, which had well developed bedforms over the entire length of the steady state region, falls very close to the measured depths. The section from 8 to 12 feet into the reservoir for the 0.47 cfs flow, which also contained bedforms, also fits very well, while the first 8 feet of the reservoir, which had a plane bed, deviates the most.

When the bed profile model was tested, sensitivity studies showed that the predicted bed profile was relatively sensitive to the flow rate that was specified. A rather small change in the flow rate seemed to produce a disproportionately large change in the bed profile. Since the measured flow rates during the experimental work did vary by several hundredths of a cubic foot per second, some of the deviation of the

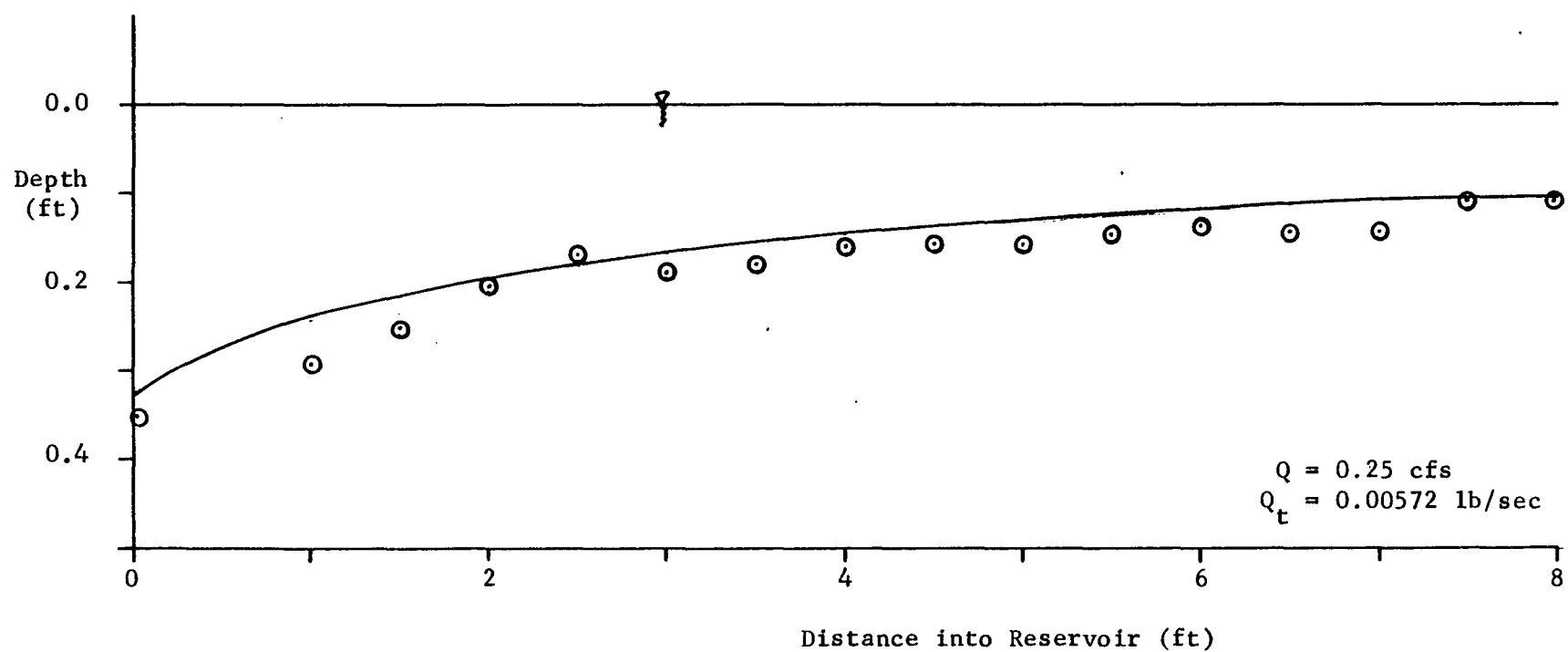


Figure 5.1 Predicted and Measured Bed Profiles

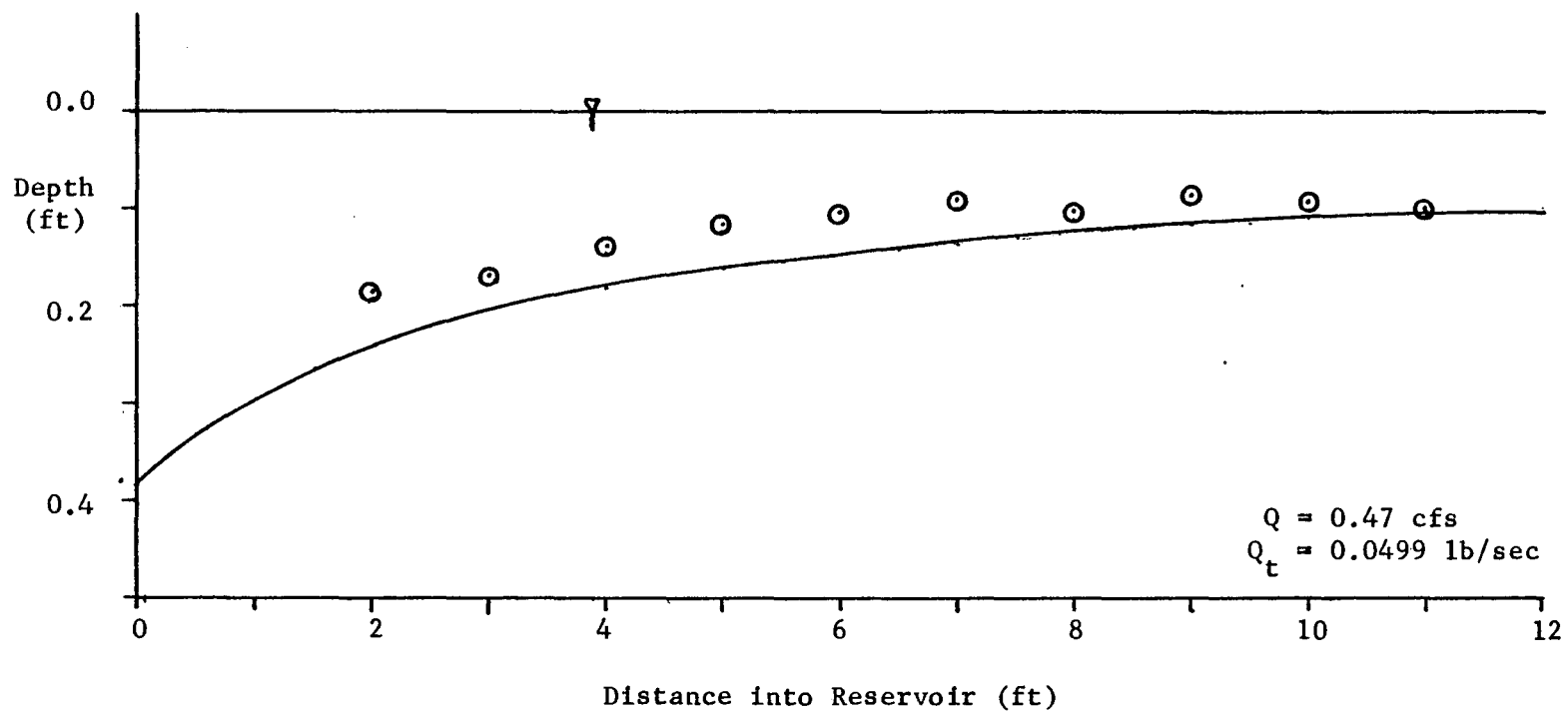


Figure 5.2 Predicted and Measured Bed Profiles

predictions from the experimental data may be attributed to the use of an average flow rate by the model.

Another shortcoming of the analytical model is the way in which the energy slope is calculated. Only one value of Manning's roughness coefficient is specified for the entire reservoir, and the energy slope is computed using that coefficient and the hydraulic parameters of the flow. The sensitivity analysis showed that changing the value of Manning's n did produce a small change in the predicted depths of flow. During the experimental work, it was observed that the bed form characteristics varied significantly with distance into the reservoir. The bedform heights became an increasingly larger fraction of the flow depth as the average flow depth decreased. The friction contributed by the bedforms could be expected to increase with distance into the reservoir, yet this could not be accounted for by the model. The roughness variation could be significant when modeling the laboratory reservoir, but would probably be minimal in a full scale situation. The model could be improved by using a different approach to finding the energy slope that could account for the changing friction contribution of the bedforms.

The ratio of the bedload to total load data that were measured are shown plotted with the analytical predictions in Figures 5.3 and 5.4. As would be expected, the model predicted that there would be a greater proportion of bedload at the lower flow rate. Higher flows with greater velocities would tend to carry more sediment as suspended load. However, the laboratory data taken were inconclusive. It is realized that the bedload trap was a relatively crude method for measuring the bedload transport rate and was not highly precise. Even though the trap appeared to work well,

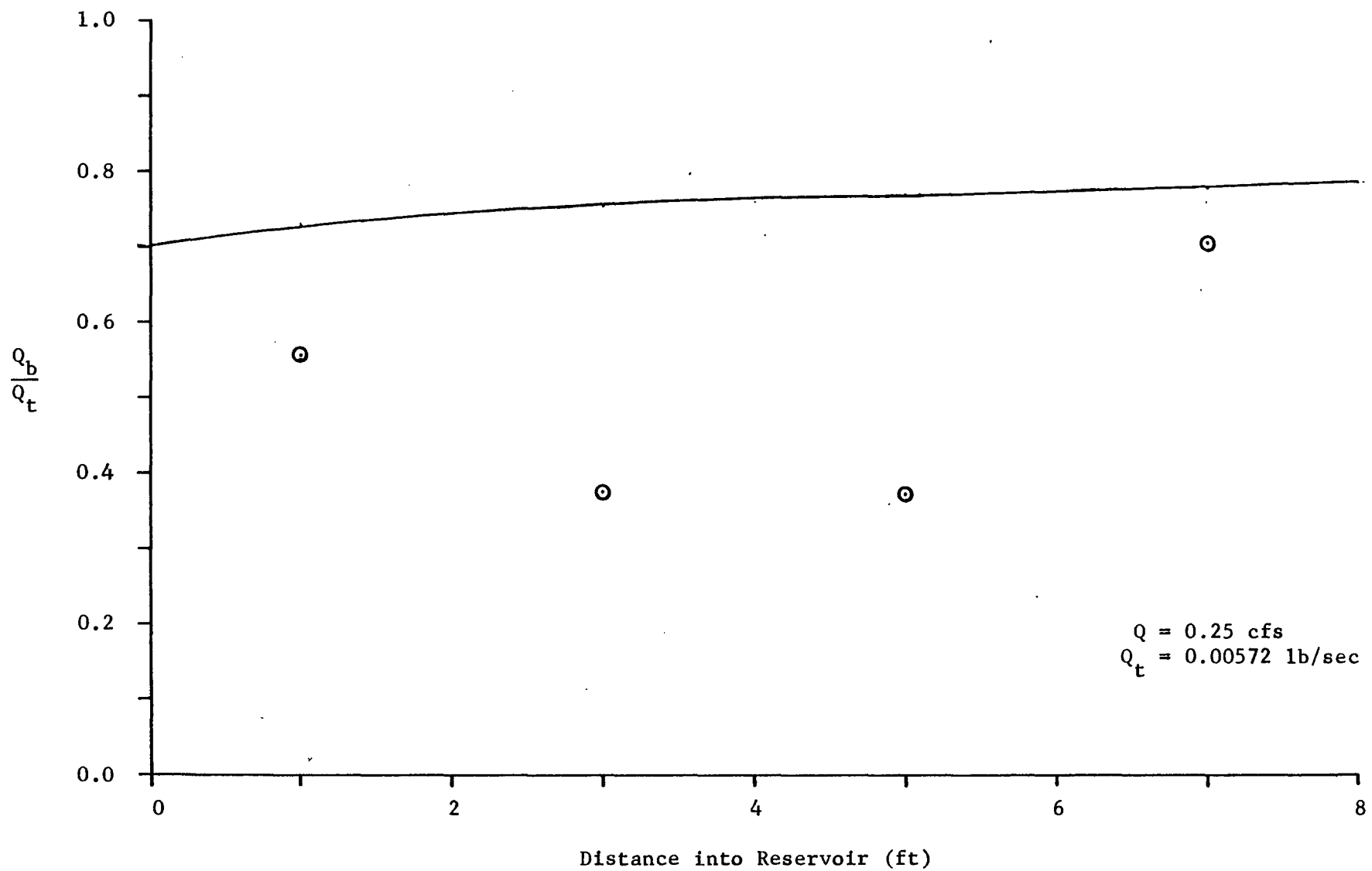


Figure 5.3 Variation of Bedload to Total Load Ratio with Distance
Theoretical Curve and Experimental Points

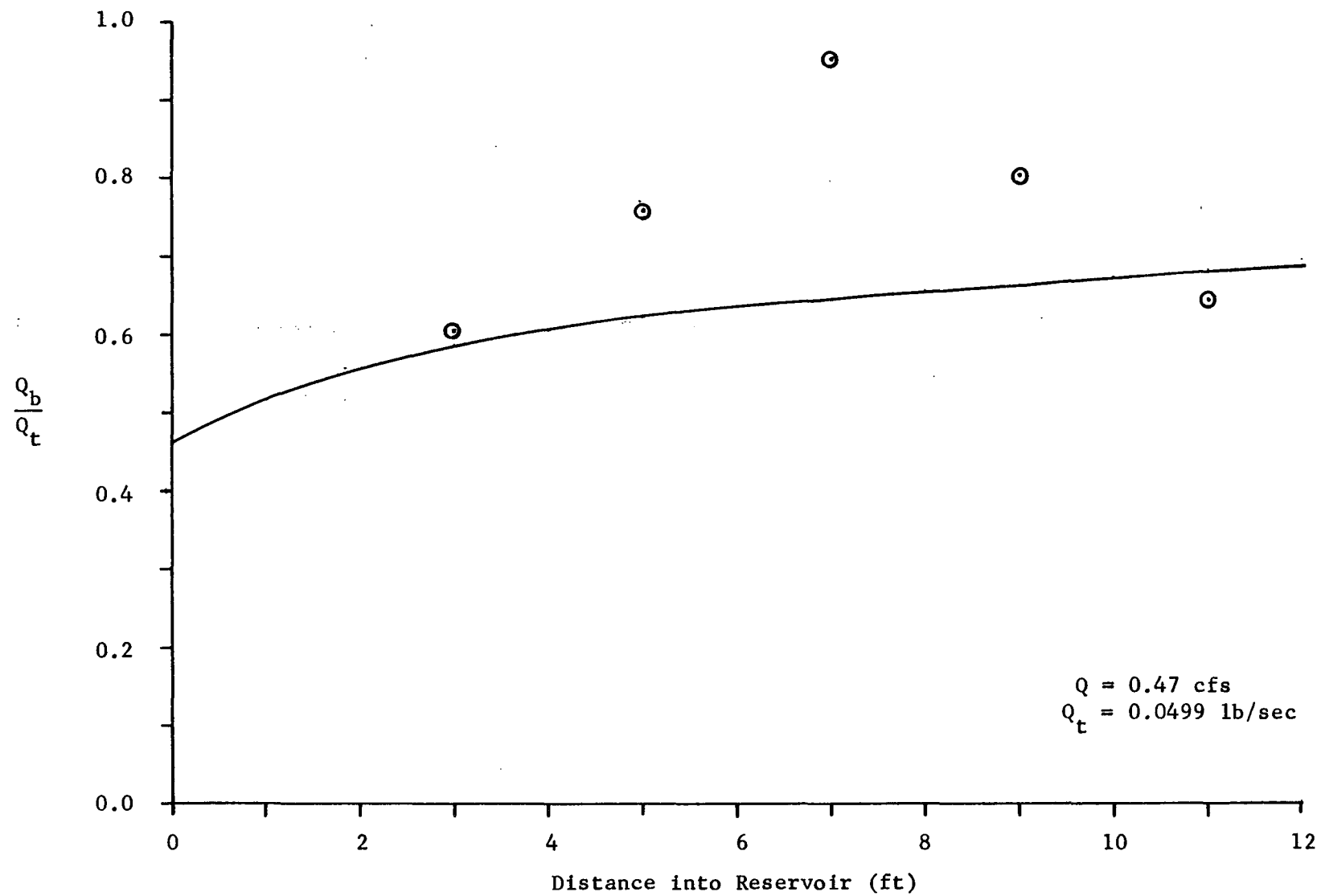


Figure 5.4 Variation of Bedload to Total Load Ratio with Distance
Theoretical Curve and Experimental Points

it is possible that small variations in its placement could have had large effects in the trap's performance.

Although the laboratory data do not fit the curves well, the possibility that the fit is not better because of random scatter cannot be disallowed. Relatively few data points were obtained during the experimental work, and they are not sufficient to draw any conclusions. Only more extensive testing can verify whether or not the model can accurately predict the proportion of bedload carried by the flow.

The assumption that a mildly nonuniform flow can be approximated by a series of uniform flow reaches creates problems in analyzing the suspended load. The model uses the uniform flow characteristics to calculate the equilibrium sediment transport conditions at the center of the reach. If the model predicts a sudden drop in the flow's capacity to carry suspended sediment, it is assumed that the suspended particles are immediately removed from the flow. In actuality, the particles will settle out of the flow over some period of time dependant on their settling velocity. This means that although the flow may not physically be able to carry some particles in suspension, they will be a part of the suspended load until they settle out some distance later. The model cannot take this into account, yet a mild change in the suspended load carrying capacity of the flow should not cause significant problems with the model's depth or bedload predictions. Certainly this topic should be the focus of further investigation.

6. SUMMARY AND CONCLUSIONS

The steady state bed profile for a mildly diverging reservoir has been studied both analytically and experimentally. For the steady state situation, the total rate of sediment transport through any cross section of the reservoir is constant, and equal to the rate of sediment transport into the reservoir. A model was developed that iterates to find the depth at any point in the reservoir that corresponds to the incoming sediment rate, and the bed profile of the reservoir can be predicted.

The key to the bed profile model was the development of a technique for directly calculating the sediment transport rate from given flow conditions using Einstein's 1950 bedload function. This technique provided the fast, direct method for calculating sediment transport rate that the bed profile model required.

A model approximated a mildly nonuniform flow with a series of uniform flow reaches. The depth corresponding to the incoming sediment transport rate could be calculated for each of the reaches, resulting in the bed profile for steady state conditions. The model was used to predict the bed profiles for two flow rates through a laboratory reservoir. The laboratory data fell very close to the predicted bed profiles, although the comparison of measurements of the bedload to total load ratio and predictions from the model was inconclusive.

As a result of this investigation, the following conclusions can be drawn:

1. A modification to Einstein's bedload function can be made which allows for the direct calculation of sediment transport rates from

specified flow conditions and sediment properties.

2. The steady state bed profile of a diverging reservoir can be predicted using Einstein's bedload function by approximating the reservoir with a series of uniform flow reaches.
3. Further research is necessary to investigate the relationship between bedload and suspended load in a decelerating flow region.

REFERENCES

1. Graf, Walter Hans (1971), HYDRAULICS OF SEDIMENT TRANSPORT, McGraw-Hill, New York.
2. Einstein, Hans Albert (1950), "The Bed-Load Function for Sediment Transport in Open Channel Flows", U.S. Department of Agriculture, Technical Bulletin No. 1026.
3. Vanoni, V. A. and Brooks, N. H. (1957), LABORATORY STUDIES OF THE ROUGHNESS AND SUSPENDED LOAD OF ALLUVIAL STREAMS, California Institute of Technology Sedimentation Laboratory, Pasadena, California.
4. Simons and Richardson (1966), "Resistance to Flow in Alluvial Channels," Geological Survey Professional Paper 422-J.
5. National Bureau of Standards (1970), HANDBOOK OF MATHEMATICAL FUNCTIONS WITH FORMULAS, GRAPHS, AND MATHEMATICAL TABLES, U.S. Government Printing Office, Washington, D. C.
6. Keulegan, G. H. (1938), "Laws of Turbulent Flow in Open Channels," Natl. Bureau of Standards, Jour. Res., vol 21, 1938, pp 701-741.

APPENDIX I - DIRECT EINSTEIN COMPUTER PACKAGE

This group of computer subroutines was written to directly compute sediment transport rates for known flow conditions following the method described in Einstein's 1950 paper (2) as closely as possible. The theory behind the direct computation method has been outlined in Chapter 3. Comparison of the computer results to those found by Einstein is presented in Appendix II.

The subroutines were written for and run on the CDC digital computer at Lehigh University, using the FTN compiler with an optimization parameter of 2. The programming was done in ANSI FORTRAN IV, so that modifications needed to run the package on a different computer system should be minimal.

The input parameters for use of the subroutines are as follows:

- D diameter (in feet) of the sediment particle for which sediment transport calculations are to be performed
- VS settling velocity of the particle. This can be determined by a call to subroutine VSETTL, which uses Rubey's settling velocity equation.
- D35 diameter of particle in a sediment mixture for which 35 percent of the mixture is smaller
- D65 65 percent finer grain diameter
- SGS specific gravity of the sediment
- V velocity of flow, in feet per second
- SE energy slope of the flow
- RB hydraulic radius of the flow with respect to the bed
- RT total hydraulic radius of the flow. For other than wide channels, the depth should be specified.
- IP print parameter, as described in the program.

If these parameters are specified in a call to subroutine SEDFLO, the hydraulic radius with respect to the bed due to grain roughness, R'_b , will be determined and the total sediment transport rate and bedload transport rate will be calculated.

If R'_b has been previously determined, for instance, through sediment rate calculations for the same flow conditions but with a different sediment size, the entry point SEDRB can be used with the same formal parameters as a call to SEDFLO. Specifying RBP in a call to SEDRB eliminates the iteration process to calculate RBP, but is otherwise identical to a call to SEDFLO.

The listing of the subroutines in the computer package follow. Comment cards have been placed wherever necessary to help the user. The equations used to fit the curves for the correction factors x , y , and ξ as well as the error function relationship between Φ_* and Ψ_* are shown after the listing.

SUBROUTINE SEDFLO(D,VS,V,SE,RB,RBP,RT,D35,D65,SGS,QT,QB,IP)

SEDFLO IS A SEDIMENT TRANSPORT ROUTINE BASED ON EINSTEIN'S 1950 PAPER. GIVEN THE PHYSICAL CHARACTERISTICS OF THE FLOW, IT WILL CALCULATE DIRECTLY THE BED AND TOTAL LOADS, RATHER THAN DEVELOPING RATING CURVES FOR ALL FLOWS.

THE FORMAL PARAMETERS OF SEDFLO ARE LISTED BELOW.

FORMAL PARAMETERS

D SEDIMENT PARTICLE DIAMETER
 VS SETTLING VELOCITY OF PARTICLE
 V AVERAGE VELOCITY OF FLOW
 SE ENERGY SLOPE
 RB HYDRAULIC RADIUS WITH RESPECT TO BED
 RBP HYDRAULIC RADIUS DUE TO GRAIN ROUGHNESS
 RT TOTAL HYDRAULIC RADIUS OF THE FLOW
 (FOR OTHER THAN WIDE CHANNELS, USE DEPTH)
 D35 ... 35 PERCENT FINER GRAIN DIAMETER
 D65 ... 65 PERCENT FINER GRAIN DIAMETER
 SGS ... SPECIFIC GRAVITY OF SEDIMENT
 QT CALCULATED TOTAL SEDIMENT TRANSPORT (LB/FT/SEC)
 QB CALCULATED BEDLOAD TRANSPORT (LB/FT/SEC)
 IP PRINT PARAMETER 0 = DO NOT PRINT
 1 = PRINT RESULTS

FOR CALLS TO SEDFLO, VALUES MUST BE PROVIDED FOR ALL PARAMETERS EXCEPT RBP, QT, AND QB. (THE PARTICLE SETTLING VELOCITY, VS, MAY BE DETERMINED BEFOREHAND BY USE OF SUBROUTINE VSETTL.) SEDFLO WILL CALCULATE THE VALUE OF RBP APPROPRIATE TO THE FLOW CONDITIONS, AND WILL THEN DETERMINE QB AND QT. A SUMMARY OF THE CALCULATED DATA WILL BE PROVIDED IF THE PRINT OPTION IS SPECIFIED.

IF RBP IS KNOWN OR HAS BEEN PREVIOUSLY DETERMINED BY A CALL TO SEDFLO, ENTRY POINT SEDRB MAY BE USED. THIS WILL ELIMINATE THE ITERATION PROCESS WHICH CALCULATES RBP. SEDRB DOES NOT REQUIRE VALUES FOR V OR RB. HOWEVER, IF THE PRINTING OPTION IS SPECIFIED, VALUES SHOULD BE PROVIDED.

ADDITIONAL INFORMATION ON THE DEVELOPMENT OF SEDFLO IS AVAILABLE IN THE DOCUMENTATION.

REAL NU,I1,I2

..... DEFAULT VALUES FOR THE MEMBERS OF COMMON BLOCKS TAPES,E1, AND E2 HAVE BEEN SPECIFIED IN BLOCK DATA.

COMMON/TAPES/IR,IM
 COMMON/E1/G,NU,RHO,GAMMA
 COMMON/E2/TOL,MAX

..... COMMON BLOCK JUNK HAS BEEN ORDERED SO THAT CALCULATIONS PERFORMED BY SEDFLO TAKE UP THE MINIMUM AMOUNT OF CORE STORAGE. ANY CHANGES MADE TO THIS BLOCK MAY CAUSE SOME OVERWRITING OF CORE AND PRODUCE INCORRECT RESULTS.

COMMON/JUNK/A,DELTA,USTARP,S1,X,I1,I2,DELT,Z,PHI,PSI,B,Y,U,CHK,
 2 CHI,ZETA,S,X1,X2,I,QQ
 EQUIVALENCE (I,P),(DELT,K)

THE EXPRESSIONS SE*G AND SGS-1. ARE FREQUENTLY USED, SO THEIR VALUES ARE STORED TO PREVENT REPETITIVE CALCULATIONS.

S=SE*G
 S1=SGS-1.

```

ITERATE TO FIND THE VALUE OF RBP, THE HYDRAULIC RADIUS DUE TO THE
GRAINS, WHICH SATISFIES THE REQUIRED VELOCITY PROFILE. THE
ITERATION IS DONE BY THE METHOD OF BISECTION, KNOWING THAT RBP
MUST BE BETWEEN 0. AND RB, SINCE RB PRIME AND RB DOUBLE PRIME
MUST SUM TO GIVE RB, THE TOTAL HYDRAULIC RADIUS WITH RESPECT TO
THE BED.

THE MAXIMUM RELATIVE ERROR ( TOL ) AND MAXIMUM NUMBER OF ITERATIONS
ALLOWED ARE SPECIFIED IN BLOCK DATA, COMMON BLOCK E2.

X1=RB
X2=0.

DO 40 I=1,MAX
RBP=(X1+X2)/2.
U*PRIME IS THE SHEAR VELOCITY DUE TO GRAIN ROUGHNESS
USTARP=SQRT(S*PRIME)
DELTA IS THE THICKNESS OF THE LAMINAR SUBLAYER FOR SMOOTH WALLS
DELTA=11.6*NU/USTARP
DETERMINE VELOCITY DISTRIBUTION CORRECTION FACTOR X
CALL CFX(X,065,DELTA)
DELT IS THE APPARENT BED ROUGHNESS
DELT=065/X
CALCULATE VELOCITY FOR THIS VALUE OF RBP
EQTN. 9 PG. 10 EINSTEIN 1950
U=USTARP*5.75*ALOG10(12.27*RBP/DELT)
IF CALCULATED VELOCITY DOES NOT AGREE WITH ACTUAL VELOCITY, ADJUST RBP
CHK=ABS((V-U)/V)
IF(CHK.LT.TOL)50,10
IF(U.GT.V)20,30
10 X1=RBP
20 X2=RBP
30 X1=RBP
40 CONTINUE

ERROR MESSAGE IF CONVERGENCE NOT REACHED IN MAX ITERATIONS
WRITE(1M,1510)MAX,RBP,RB
STOP 1000

*****
ENTRY SEDRB
*****

THIS ENTRY POINT MAY BE USED IF THE HYDRAULIC RADIUS DUE TO GRAIN
ROUGHNESS, RB PRIME( RBP ), IS KNOWN OR HAS BEEN PREVIOUSLY
CALCULATED BY A CALL TO SEDFLO. THE PARAMETER LIST FOR THE CALL IS
IDENTICAL TO THAT FOR SEDFLO, AND THE VALUE OF RBP MUST BE
PROVIDED THROUGH THE PARAMETER LIST.

S1=SGS-1.
USTARP=SQRT(G*SE*RBP)
DELTA=11.6*NU/USTARP
CALL CFX(X,065,DELTA)
DELT=065/X

50 CONTINUE
Z = EXPONENT ON SUSPENDED LOAD INTEGRALS
Z=VS/0.4/USTARP
A = DIMENSIONLESS LOWER LIMIT OF SUSPENDED LOAD
A=2.*0/RT
CALCULATE SUSPENDED LOAD INTEGRALS
CALL INT(A,Z,11,12)

DETERMINE CHI -- THE CHARACTERISTIC GRAIN SIZE OF THE MIXTURE
A=DELT/DELTA
IF(A.GT.1.8)60,65
60 CHI=0.77*DELT
GO TO 70
65 CHI=1.39*DELTA

```

```

C
C      CALCULATE B/B WHERE  $B_x = \log_{10} \left[ \frac{10.6 * CHI}{DELT} \right]$ 
C
70 B=ALOG10(10.6)
   B=B/ALOG10(10.6*CHI/DELT)
C
C      DETERMINE LIFT AND HIDING CORRECTION FACTORS Y AND ZETA
C      CALL CFYZ(ZETA,Y,0,065,DELTA,CHI)
C
C       $PSI = \frac{[SGS - 1] * D}{SE * RB \text{ PRIME}}$ 
C
C       $PSI* = ZETA * Y [B/B]^2 * PSI$ 
C
C      PSI=S1*D/RBP/SE
C      PSI=ZETA*Y*B*B*PSI
C
C      FIND PHI* WHICH CORRESPONDS TO CALCULATED PSI*
C      CALL PSTAR(PSI,PHI)
C
C      QB IS BEDLOAD [LB/SEC/FT] EQTN. 42 PG. 34 EINSTEIN 1950
C      P IS THE PARAMETER OF TOTAL TRANSPORT EQTN. 62 PG. 40 EINSTEIN 1950
C      QT IS TOTAL LOAD [LB/SEC/FT] EQTN. 63 PG. 40 EINSTEIN 1950
C
C      QB=PHI*RHO*SGS*SQRT(S1)*(G**1.5)*(D**1.5)
C      P=ALOG10(30.2*X*RT/065)/0.434
C      QT=QB*(P*I1+I2+1.)
C
C      PRINTING OPTION
C
C      K=IP+1
C      GO TO (80,90),K
80 RETURN
90 WRITE(IW,1500)O,V,USTARP,DELTA,QT,035,SE,RBP,P,QB,065,RB,PSI,I1,
   2VS,RT,PHI,I2
   RETURN
C
1500 FORMAT(2(/),15X,6H0 =,E10.3,2X,7HVEL =,E10.3,2X,7H035 =,E10.
2.3,2X,8HDELTA =,E10.3,4X,5HQT =,E10.3,/,15X,6H035 =,E10.3,2X,7H
3SE =,E10.3,2X,7H065 =,E10.3,2X,8HP =,E10.3,4X,5HQB =,E1
40.3,/,15X,6H065 =,E10.3,2X,7H065 =,E10.3,2X,7HPSI* =,E10.3,2X,
58HI1 =,E10.3,/,15X,6HVS =,E10.3,2X,7HDPH =,
6,E10.3,2X,7HPHI* =,E10.3,2X,8HI2 =,E10.2,2(/))
1510 FORMAT(4(/),10X,52HWARNING -- HYDRAULIC RADIUS DOES NOT CONVERGE A
2FTER ,I3,12H ITERATIONS.,/,30X,25HLAST RB PRIME COMPUTED =,E10.3,
3/,40X,15HTOTAL RADIUS =,E10.3,/,10X,15HPROGRAM STOPPED,4(/))
   END

```

```

C      BLOCK DATA
C      REAL NU
COMMON/TAPES/IR,IW
COMMON/E1/G,NU,RHO,GAMMA
COMMON/E2/TOL,MAX
C
C...   DEFAULT VALUES FOR INPUT AND OUTPUT FILES
C      INPUT  ( IR ) = 5
C      CUTPUT ( IW ) = 6
C...   PHYSICAL PARAMETERS
C      G      = 32.17      FT/SEC/SEC
C      NU     = 1.0E-05    SQ.FT./SEC
C      RHO    = 1.94      SLUGS/CU.FT.
C      GAMMA  = 62.4      LB/CU.FT.
C...   ITERATION PARAMETERS
C      TOL = 0.0005      MAXIMUM RELATIVE ERROR
C      MAX = 25          MAXIMUM ITERATIONS TO CONVERGENCE
C...   THESE VALUES MAY BE CHANGED BY USE OF A REPLACEMENT STATEMENT IN ANY
C      ROUTINE CONTAINING THE APPROPRIATE COMMON BLOCK.
C
C      DATA IR,IW/5,6/
C      DATA G,NU,RHO,GAMMA/32.17,1.0E-05,1.94,62.4/
C      DATA TOL,MAX/0.0005,25/
C
C      END

```



```

C      SUBROUTINE VSETTL(D,VS,SGS)
      REAL NU
      COMMON/E1/G,NU,RHO,GAMMA
      COMMON/JUNK/C1,C2,C3,F0,Q(18)

C      ...  SUBROUTINE VSETTL WILL CALCULATE THE TERMINAL SETTLING VELOCITY OF A
C      ...  PARTICLE USING THE RUBEY EQUATION. THIS ROUTINE SHOULD BE
C      ...  CALLED BEFORE THE INITIAL CALL TO SEDFLO, ONCE FOR EACH
C      ...  PARTICLE DIAMETER BEING USED. THE SETTLING VELOCITY VS IS
C      ...  PROVIDED TO SEDFLO THROUGH THE PARAMETER LIST.

C      ...  VSETTL SHOULD NOT BE CALLED BEFORE EVERY CALL TO SEDFLO IF MORE THAN
C      ...  ONE CALCULATION WITH THE SAME DIAMETER PARTICLE IS PERFORMED.
C      ...  IN SUCH A CASE, VS SHOULD BE STORED TO AVOID REDUNDANT CALCULATION

C      -----
C      RUBEY EQUATION FOR SETTLING VELOCITY
C      VS = F0 * SQRT( D * G * ( SGS - 1 ) )
C      F0 = SQRT( 2/3 + C3 ) - SQRT( C3 )
C      C3 = 
$$\frac{36 * NU^2}{G * D^3 * ( SGS - 1 )}$$

C      SGS = SPECIFIC GRAVITY OF PARTICLE
C      -----

C      PHYSICAL PARAMETERS G AND NU ARE PROVIDED THROUGH COMMON BLOCK E1,
C      WHICH HAS DEFAULT VALUES SUPPLIED IN BLOCK DATA.

C      C1=(SGS-1.)*G*D
C      C2=C1*D*D
C      C3=36.*NU*NU/C2
C      F0=SQRT(2./3.+C3)-SQRT(C3)
C      VS=F0*SQRT(C1)

C      RETURN
      END

```

SUBROUTINE CFX(X,D65,DELTA)

COMMON/JUNK/A,Q(21)

... X IS A CORRECTION FACTOR USED IN THE VERTICAL VELOCITY DISTRIBUTION TRANSITION BETWEEN HYDRAULICALLY SMOOTH AND ROUGH BOUNDARIES. THE TRANSITION IS DESCRIBED BY

$$\frac{U(Y)}{U^*} = 5.75 * \log_{10} \left(30.2 \frac{Y * X}{KS} \right) = 5.75 * \log_{10} \left(30.2 \frac{Y}{DELTA} \right)$$

U(Y) = AVERAGE VELOCITY A DISTANCE Y FROM THE BED

U* = SHEAR VELOCITY

Y = DISTANCE (VERTICAL) FROM THE BED

KS = ROUGHNESS OF THE BED (TAKEN AS D65)

X = CORRECTION FACTOR, A FUNCTION OF KS / DELTA
GIVEN BY FIG. 1, EINSTEIN 1950

DELTA = THICKNESS OF THE LAMINAR SUBLAYER FOR A SMOOTH WALL

DELT = KS / X , THE APPARENT ROUGHNESS OF THE BED

THIS ROUTINE RETURNS X AS A FUNCTION OF D65 / DELTA. THE FUNCTION IS BROKEN INTO FOUR REGIONS, THE FIRST AND LAST OF WHICH ARE DESCRIBED EXACTLY. THE OTHER TWO REGIONS ARE APPROXIMATED BY CURVES TO GIVE A GOOD REPRESENTATION OF FIG. 1.

```

A=D65/DELTA
IF(A.LE..2)1,2
1 X=3.476*A
RETURN
2 IF(A.LE.2.)3,4
3 A=3.016*ALOG10(A)+1.571
X=0.62*SIN(A)+1.
RETURN
4 IF(A.LE.10.)5,6
5 A=1.-ALOG10(A)
X=A*A*.78076+1.
RETURN
6 X=1.
RETURN

```

END

```

C      SUBROUTINE CFYZ(Y,Z,D,D65,DELTA,CHI)
C      COMMON/JUNK/A,Q(21)

C      Y AND ZETA ARE CORRECTION FACTORS SUGGESTED BY EINSTEIN. THE
C      FUNCTIONS DESCRIBING Y AND ZETA ( CALLED Z IN THIS ROUTINE ) HAVE
C      BEEN BROKEN DOWN INTO A SERIES OF CURVES AND ARE APPROXIMATED
C      AS CLOSELY AS POSSIBLE.

C      SMALL PARTICLES HIDE BETWEEN LARGER ONES OR IN THE LAMINAR SUBLAYER,
C      SO THAT THEIR LIFT MUST BE CORRECTED BY 1/ZETA. ZETA, THE HIDING
C      FACTOR, IS DESCRIBED AS A FUNCTION OF D / CHI GIVEN BY FIG. 7
C      IN EINSTEIN 1950.

C      D = PARTICLE DIAMETER
C      CHI = CHARACTERISTIC GRAIN SIZE OF MIXTURE

C      THE CORRECTION FACTOR Y DESCRIBES THE CHANGE IN LIFT COEFFICIENT IN
C      MIXTURES OF VARIOUS ROUGHNESSES. THIS IS A FUNCTION OF KS / DELTA
C      AS SHOWN IN FIG. 8 OF EINSTEIN 1950.

C      KS = ROUGHNESS DIAMETER, TAKEN AS D65
C      DELTA = THICKNESS OF LAMINAR SUBLAYER FOR A SMOOTH WALL

C      FOR UNIFORM GRAINS, BOTH Y AND ZETA ARE UNITY.

C      A=D65/DELTA
C      IF (A.LT..6) 1,2
1 Y=1.05*A**1.21
C      GO TO 5
C      IF (A.LE.1.6) 3,4
2 IF (A.LE.1.6) 3,4
3 A=4.*ATAN(1.)*(1.92*ALOG10(A)+.423)
Y=.3*SIN(A)+.57
C      GO TO 5
4 A=-(7.33*ALOG10(A)-1.5)
Y=10.**(.16*EXP(A)-.284)

C      5 A=D/CHI
C      IF (A.LT..63) 6,7
6 Z=0.7*A**(-2.4)
C      GO TO 10
7 IF (A.LT.1.4) 8,9
8 A=ALOG10(1.4/A)
Z=10.**(-2.78356*A*A)
C      GO TO 10
9 Z=1.
10 RETURN

C      END

```

```

C      SUBROUTINE PSTAR(PHI,PSI)
COMMON/JUNK/Q(16),P,F,QQ(4)
...    SUBROUTINE PSTAR RELATES PHI* TO ITS CORRESPONDING VALUE OF PSI* IN
        TERMS OF AN ERROR FUNCTION. THE RELATIONSHIP IS

$$\text{PHI}^* = \frac{1}{A^*} \frac{P}{1-P}$$


$$P = 1 - 0.5 [ \text{ERF}(X1) + \text{ERF}(X2) ]$$


$$X1 = (B^*)(\text{PSI}^*) - 1/\text{ETA}$$


$$X2 = (B^*)(\text{PSI}^*) + 1/\text{ETA}$$

...    THE ERROR FUNCTION IS EVALUATED BY FUNCTION SUBPROGRAM ERF.
C      F=0.143*PSI
C      P=1.-0.5*(ERF(F+2.)+ERF(F-2.))
C      PHI=P/(1.-P)/43.5
C      RETURN
C      A* = 43.5      GRAF PG. 149
C      B* = 0.143     GRAF PG. 149
C      1/ETA = 2       GRAF PG. 149
C      END

```

```

C      FUNCTION ERF(X)
COMMON/JUNK/Q(18),EX,T,T2,T3
...    APPROXIMATION FOR ERROR FUNCTION

$$\text{ERF}(X) = 1 - [ A1 * T + A2 * T^2 + A3 * T^3 ] * \text{EXP}(-X^2)$$


$$T = \frac{1}{1 + P * X}$$


$$P = 0.47047$$


$$A1 = 0.34802 \ 42$$


$$A2 = -0.09587 \ 98$$


$$A3 = 0.74785 \ 56$$

...    APPROXIMATION IS GOOD TO WITHIN +/- 2.5 E-05
C      T=1./(1.+0.47047*ABS(X))
C      T2=T*T
C      EX=EXP(-X*X)
C      T3=1.-(0.3480242*T-0.0958798*T2+0.7478556*T*T2)*EX
C      ERF=SIGN(T3,X)
C      RETURN
C      END

```

```

C      SUBROUTINE INT(A,Z,I1,I2)
C      REAL I1,I2
C      COMMON/TAPES/IR,IM
C      COMMON/JUNK/Q(9),DX,I,J,N,X1,X2,F,QQ(6)

          EVALUATION OF SUSPENDED LOAD INTEGRALS

...    THE INTEGRALS I1 AND I2 ARE DEFINED BY

          I1 = F * J1
          I2 = F * J2

          F = 0.216 *  $\frac{A^{(Z-1)}}{(1-A)^Z}$ 

          WHERE A = DIMENSIONLESS LOWER LIMIT OF SUSPENDED LOAD,  $\frac{Z * 0}{\text{DEPTH}}$ 
          Z = VS / ( 0.4 * U* PRIME )

          J1 = THE INTEGRAL OF  $\left[ \frac{1-Y}{Y} \right]^Z$  DY
          J2 = THE INTEGRAL OF  $\left[ \frac{1-Y}{Y} \right]^Z \ln(Y)$  DY

...    THE J1 AND J2 INTEGRALS ARE EVALUATED BY SIMPSONS RULE, AS SUGGESTED
          IN EINSTEIN 1950 ( PG. 19 - 24 ). THE INTEGRALS ARE EVALUATED
          STARTING AT THE UPPER LIMIT ( 1 ) AND THE INCREMENTAL ELEMENT OF
          INTEGRATION SIZE IS DECREASED AS THE INTEGRATION APPROACHES THE
          LOWER LIMIT ( A ). SUBROUTINE INT DETERMINES THE APPROPRIATE SIZE
          AND NUMBER OF ELEMENTS TO BE USED, AND TRANSFERS CONTROL TO
          SUBROUTINE SIMP, WHICH PERFORMS THE ACTUAL SIMPSONS RULE.

C      INTEGRALS NOT EVALUATED FOR A LESS THAN 1. E-05
C      IF (A.LT.1.E-5) GO TO 10
C      X1 IS CURRENT UPPER LIMIT OF INTEGRATION
C      10 X1=1.
C      INITIALIZE INTEGRAL SUMMATIONS TO ZERO
C      I1=0.
C      I2=0.
C      DO 40 I=1,5
C      SET STEP SIZE FOR J = 1
C      N=20
C      DX=0.4
C      DO 30 J=1,2
C      COUNTER J CONTROLS VARIABLE STEP SIZE ( DX )
C      J = 1      INTEGRATE FROM  $10 * 10^{-I}$  TO  $2 * 10^{-I}$  IN 10 STEPS
C      J = 2      INTEGRATE FROM  $2 * 10^{-I}$  TO  $1 * 10^{-I}$  IN 5 STEPS
C      DX=DX*10.**(-I)
C      X2 IS LOWER LIMIT OF INTEGRATION FOR THIS STEP SIZE
C      X2=X1-FLOAT(N)*DX
C      IF X2 IS LESS THAN A, STEP SIZE IS TOO LARGE
C      IF (X2.LE.A) GO TO 20
C      PERFORM INTEGRATION FROM X1 TO X2
C      20 CALL SIMP(X1,N,DX,Z,I1,I2)
C      CHANGE STEP SIZE FOR J = 2
C      N=10
C      30 DX=0.1
C      40 CONTINUE
C

```

```

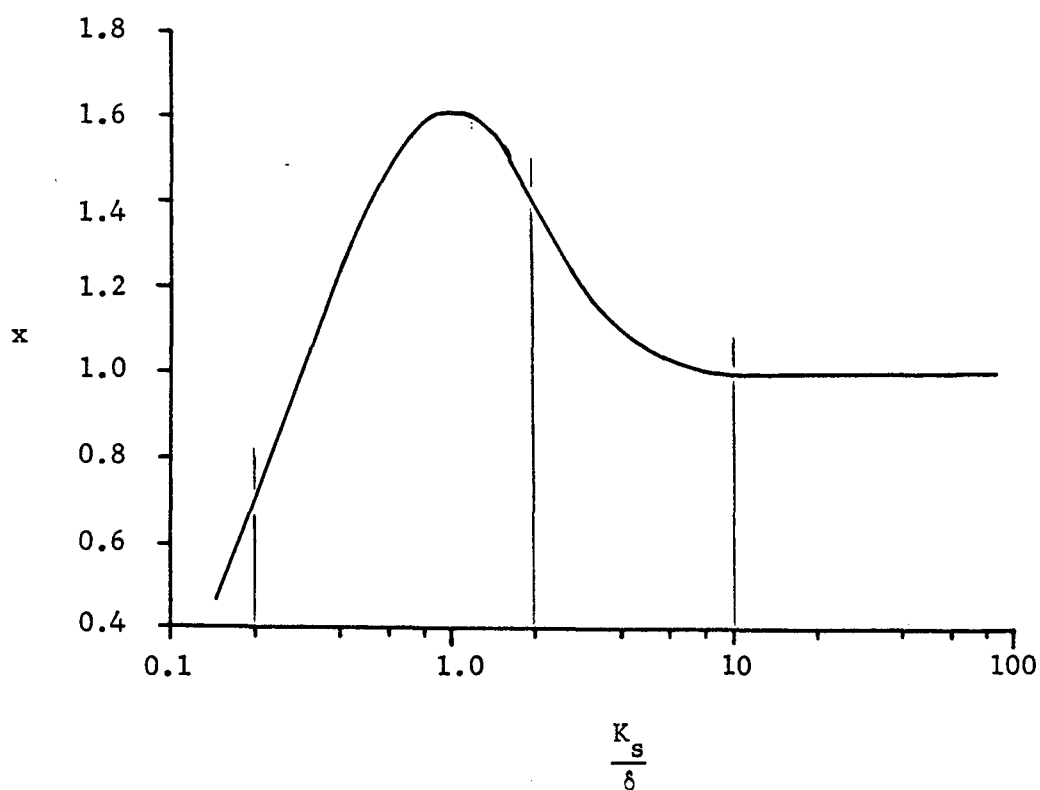
C   CALCULATE STEP SIZE SO THAT 10 INTERVALS END EXACTLY AT LOWER LIMIT A
50 N=20
   DX=(X1-A)/FLOAT(N)
   CALL SIMP(X1,N,DX,Z,I1,I2)
C   INTEGRALS RETURNED ARE ACTUALLY J1 AND J2.  CALCULATE F AND FIND PRODUCT
C   TO GET I1 AND I2.
   F=.216*A**((Z-1.)/(1.-A)**Z
   I1=I1*F
   I2=I2*F
   RETURN
C   ERROR MESSAGE
60 WRITE(IN,1500)A
1580 FORMAT(5(/),10X,57HWARNING -- A VERY SMALL.  INTEGRALS NOT EVALUA
      TED.  A = ,E10.3,4(/))
      STOP 3000
      END

```

```

      SUBROUTINE SIMP(X,N,DX,Z,SUM1,SUM2)
C
C   REAL J1,J2
C   COMMON/JUNK/Q(14),I,K,J1(3),J2(3)
C
C   FUNCTION F IS THE EXPRESSION WHICH YIELDS J1 WHEN INTEGRATED
C   F(A,B)=((1.-A)/A)**B
C
C   J1(1)=F(X,Z)
C   J2(1)=J1(1)*ALOG(X)
C
C   PERFORM INTEGRATION OVER N/2 SUBAREAS
C   DO 20 I=1,N,2
C   EVALUATE FUNCTIONS FOR J1 AND J2 AT 3 POINTS DX APART
C   DO 10 K=2,3
C   X=X-DX
C   J1(K)=F(X,Z)
10  J2(K)=J1(K)*ALOG(X)
C
C   APPLY SIMPSONS RULE
C   SUM1=SUM1+(J1(1)+4.*J1(2)+J1(3))*DX/3.
C   SUM2=SUM2+(J2(1)+4.*J2(2)+J2(3))*DX/3.
C
C   LAST VALUES OF J1 AND J2 BECOME THE FIRST VALUES FOR THE NEXT INTEGRATION
C   J1(1)=J1(3)
C   J2(1)=J2(3)
20  CONTINUE
      RETURN
      END

```

Correction Factor x Figure AI.1 Correction Factor x

The curve describing the relationship between x , the correction factor in the vertical velocity distribution between hydraulically smooth and rough boundaries, and K_s/δ has been approximated by the following curves:

$K_s/\delta \leq 0.2$	$x = 3.476 * K_s/\delta$
$0.2 < K_s/\delta \leq 2.0$	$x = 1.0 + 0.62 * \sin[3.016 * \log_{10}(K_s/\delta) + 1.571]$
$2.0 < K_s/\delta \leq 10.0$	$x = 1.0 + 0.78076 * [1.0 - \log_{10}(K_s/\delta)]^2$
$10.0 < K_s/\delta$	$x = 1.0$

Correction Factor Y

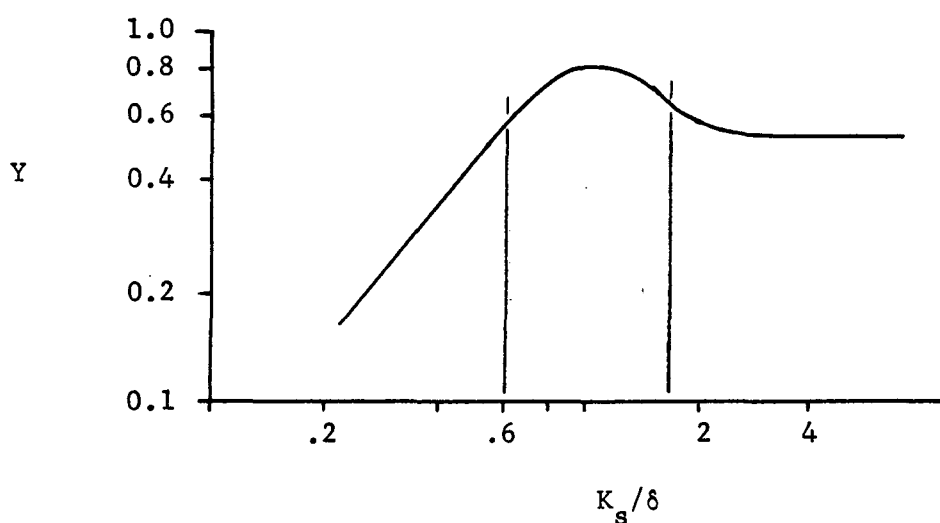


Figure AI.2 Pressure Correction in the Transition to a Smooth Bed

The correction factor Y describes the change in lift coefficients in sediment mixtures of various roughnesses. The relationship between Y and K_s/δ has been approximated by the following curves:

$K_s/\delta < 0.6$	$Y = 1.05 * (K_s/\delta)^{1.21}$
$0.6 \leq K_s/\delta \leq 1.6$	$Y = 0.3 * \sin(A) + 0.57$
	$A = \pi * [1.92 * \log_{10}(K_s/\delta) + 0.423]$
$1.6 < K_s/\delta$	$Y = 10^{(0.16 * e^A - 0.284)}$
	$A = -[7.33 * \log_{10}(K_s/\delta) - 1.5]$

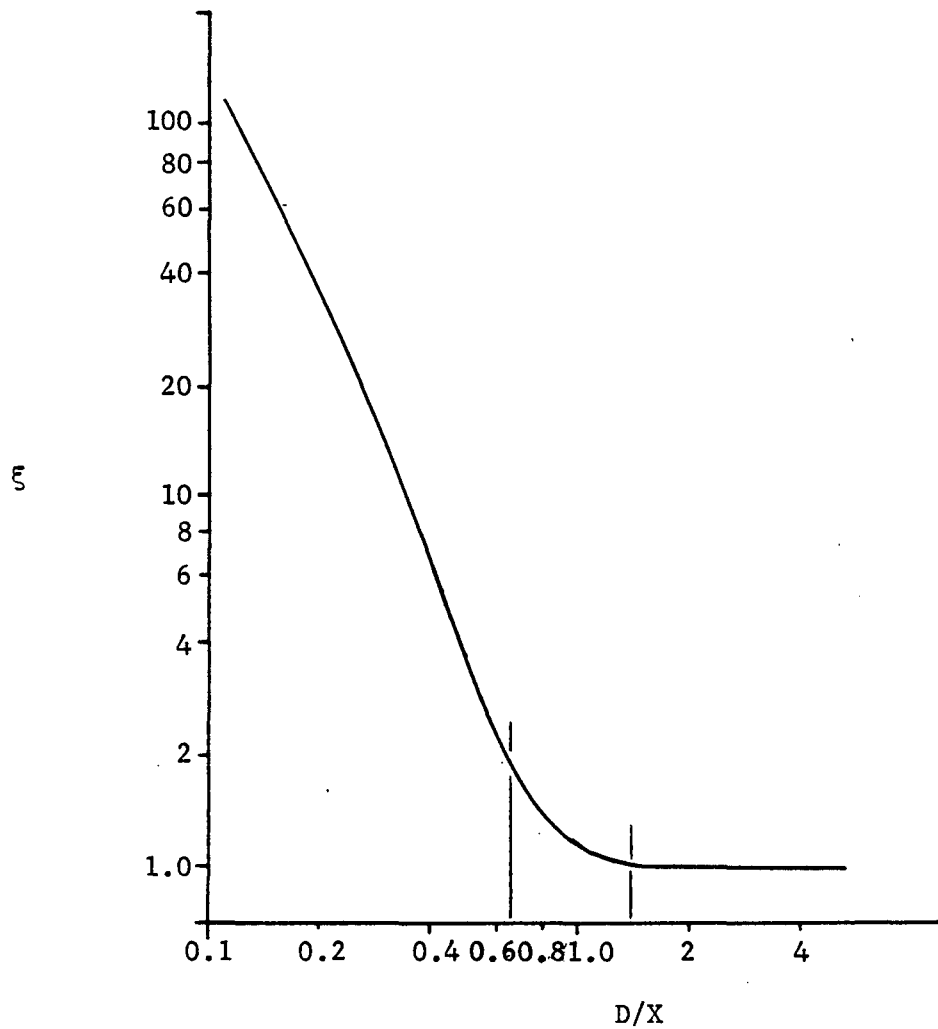
Correction Factor ξ 

Figure AI.3 Hiding Factor

The correction factor ξ is used to correct the lift for small particles which "hide" in a sediment mixture. The relationship between ξ and D/X has been approximated by:

$D/X < 0.63$	$\xi = 0.7 * (D/X)^{-2.4}$
$0.63 \leq D/X < 1.4$	$\xi = 10^{(2.78356 * A^2)}$
	$A = \log_{10}\left(\frac{1.4}{D/X}\right)$
$1.4 \leq D/X$	$\xi = 1.0$

Error Function Relationship between Φ_* and Ψ_*

The relationship between Φ_* and Ψ_* is given in Einstein's 1950 paper (2) as:

$$\frac{A_* \Phi_*}{1 - A_* \Phi_*} = P = 1 - \frac{1}{\sqrt{\pi}} \int_{-B_* \Psi_* - 1/\eta_0}^{B_* \Psi_* - 1/\eta_0} e^{-t^2} dt \quad \text{AI.1}$$

The error function, $\text{erf}(x)$, is defined by:

$$\text{erf}(x) = \frac{2}{\sqrt{\pi}} \int_0^x e^{-t^2} dt \quad \text{AI.2}$$

Rearranging Equation AI.1

$$P = 1 - \frac{1}{\sqrt{\pi}} \left[\int_0^{x_1} e^{-t^2} dt - \int_0^{x_2} e^{-t^2} dt \right] \quad \text{AI.3}$$

where

$$x_1 = B_* \Psi_* - 1/\eta_0 \quad \text{AI.4}$$

$$x_2 = -B_* \Psi_* - 1/\eta_0 \quad \text{AI.5}$$

Then

$$P = 1 - \frac{1}{2} \left[\text{erf}(x_1) - \text{erf}(x_2) \right] \quad \text{AI.6}$$

However, by definition:

$$\text{erf}(-x) = -\text{erf}(x) \quad \text{AI.7}$$

Redefining x_1 and x_2 and substituting into Equation AI.6:

$$x_1 = B_* \Psi_* + 1/\eta_0 \quad \text{AI.8}$$

$$x_2 = B_* \Psi_* - 1/\eta_0 \quad \text{AI.9}$$

$$P = 1 - \frac{1}{2} \left[\text{erf}(x_1) + \text{erf}(x_2) \right] \quad \text{AI.10}$$

Rearranging the left hand side of Equation AI.1:

$$\frac{1}{P} = \frac{1}{A_* \bar{\Phi}_*} + 1 \quad \text{AI.11}$$

$$A_* \bar{\Phi}_* = \frac{P}{1-P} \quad \text{AI.12}$$

$$\bar{\Phi}_* = \frac{1}{A_*} \frac{P}{1-P} \quad \text{AI.13}$$

Equations AI.13 and AI.10 can be used to find $\bar{\Phi}_*$ if Ψ_* is known. The universal constants A_* , B_* , and $1/\eta_0$ have been determined experimentally (), and are

$$A_* = 43.5 \quad \text{AI.14}$$

$$B_* = 0.143 \quad \text{AI.15}$$

$$1/\eta_0 = 2.0 \quad \text{AI.16}$$

An approximation for the error function good to within $\pm 2.5 \times 10^{-5}$

(5) has been used in the computer model:

$$\text{erf}(x) = 1.0 - [0.34802 \ 42t - 0.09587 \ 98t^2 + 0.74785 \ 56t^3]e^{-x^2} \quad \text{AI.17}$$

$$t = \frac{1}{1 + 0.47047 \ x} \quad \text{AI.18}$$

APPENDIX II COMPARISON OF COMPUTER PACKAGE RESULTS TO EINSTEIN'S

The direct Einstein computer package was compared to the Einstein 1950 method for calculating sediment transport rates by using input data from the example calculations in Einstein's paper (2). Since the hydraulic calculations are different for the two methods, the computer package requires R_b and V to be input, while Einstein starts with an assumed R_b' and calculates R_b and V . In order to make a direct comparison between the two methods, the values of R_b and V that Einstein calculated were used as input for the computer package. The procedures and results for each of the methods follow. It was assumed that there was no bank friction on the channel.

Hydraulic calculations for computer package

Given:	$D = 0.00162 \text{ ft}$	$S_{GS} = 2.65$
	$D_{35} = 0.00094 \text{ ft}$	$D_{65} = 0.00115 \text{ ft}$
	$S_e = 0.00105$	$i_b = 0.178$
	$R_b = 2.50 \text{ ft}$	$V = 6.63 \text{ ft/sec}$

Iterate to find R_b' , knowing that $0 \leq R_b' \leq R_b$

1. Choose R_b'
2. $u_*' = \sqrt{g S_e' R_b'}$
3. $\delta = 11.6 \sqrt{u_*'}$
4. Determine correction factor x in the transition from hydraulically smooth to rough walls as a function of D_{65}/δ
5. $\Delta = D_{65}/x$
6. $\bar{U} = u_*' 5.75 \log_{10}(12.27 R_b'/\Delta)$

If the value of \bar{U} calculate is sufficiently close to the given V , then the correct value of R_b' has been found. If not, adjust R_b' and return to Step 2.

Results: $R_b' = 2.0$ ft

$$u_*' = 0.260 \text{ ft/sec}$$

$$\delta = 0.00045 \text{ ft}$$

$$x = 1.27$$

$$\Delta = 0.00091 \text{ ft}$$

$$\bar{U} = 6.63 \text{ ft/sec}$$

Hydraulic Calculations for Einstein 1950 Method

Given: $D = 0.00162$ ft

$$S_{GS} = 2.65$$

$$D_{35} = 0.00094 \text{ ft}$$

$$D_{65} = 0.00115 \text{ ft}$$

$$S_e = 0.00105$$

$$i_b = 0.178$$

$$R_b' = 2.0 \text{ ft}$$

$$1. \quad u_*' = \sqrt{g R_b' S_e}$$

$$2. \quad \delta = 11.6 \nu / u_*'$$

3. Determine correction factor x as a function of D_{65}/δ

$$4. \quad \Delta = K_s/x$$

$$5. \quad \bar{U} = u_*' 5.75 \log_{10}(12.27 R_b'/\Delta)$$

$$6. \quad \Psi' = \frac{\rho_s - \rho}{\rho} \frac{D_{35}}{R_b' S_e}$$

7. Find \bar{u}/u_*'' from plot as a function of Ψ'

$$8. \quad u_*'' = \bar{U} / (\bar{u}/u_*'')$$

$$9. \quad R_b'' = \frac{(u_*'')^2}{S_e g}$$

$$10. \quad R_b = R_b' + R_b''$$

11. From R_b and \bar{U} , the area of flow and the flow rate can be determined using channel geometry.

Results: $u_*' = 0.259 \text{ ft/sec}$

$$\delta = 0.00047 \text{ ft}$$

$$x = 1.27$$

$$\Delta = 0.00090 \text{ ft}$$

$$\bar{U} = 6.63 \text{ ft/sec}$$

$$\Psi' = 0.75$$

$$u_*'' = 0.13 \text{ ft/sec}$$

$$R_b'' = 0.50 \text{ ft}$$

$$R_b = 2.50 \text{ ft}$$

Sediment Rate Calculations

The procedures for sediment rate calculations are identical for the two methods.

1. Determine pressure correction factor y as a function of D_{65}/δ
2. $\Delta/\delta > 1.8$ $X = 0.77\Delta$
 $\Delta/\delta \leq 1.8$ $X = 1.39\delta$
3. Determine hiding factor ξ as a function of D/X
4. $\beta = \log_{10}(10.6)$
 $\beta_x = \log_{10}(10.6 X/\Delta)$
5. $\Psi_* = \xi Y (\beta/\beta_x)^2 \left(\frac{\rho_s - \rho}{\rho} \right) \frac{D}{R_b' S_e}$
6. Determine Φ_* as a function of Ψ_*
7. $i_b q_b = i_b \Phi_* \rho_s g^{3/2} D^{3/2} \left(\frac{\rho_s - \rho}{\rho} \right)^{1/2}$
8. $z = \frac{V_s}{0.4 u_*'}$
9. $A = 2D/R_T$
10. Find suspended load integrals I_1 and I_2 as functions of A and z

$$11. \quad P = \frac{1}{0.434} \log_{10} \left(\frac{30.2 \times R_T}{D_{65}} \right)$$

$$12. \quad i_T q_T = i_b q_b (P I_1 + I_2 + 1)$$

RESULTS

	Einstein 1950	Computer Package
1.	$Y = 0.56$	$Y = 0.56$
2.	$X = 0.00069 \text{ ft}$	$X = 0.00070 \text{ ft}$
3.	$\xi = 1.00$	$\xi = 1.00$
4.	$(B/B_x)^2 = 1.27$	$(B/B_x)^2 = 1.26$
5.	$\Psi_* = 0.90$	$\Psi_* = 0.91$
6.	$\Phi_* = 8.2$	$\Phi_* = 8.22$
7.	$i_b q_b = 0.115 \text{ lb/sec/ft}$	$i_b q_b = 0.115 \text{ lb/sec/ft}$
8.	$z = 1.88$	$z = 1.97$
9.	$A = 0.00130$	$A = 0.00130$
10.	$I_1 = 0.240$	$I_1 = 0.219$
	$I_2 = -1.27$	$I_2 = -1.239$
11.	$P = 11.30$	$P = 11.34$
12.	$i_T q_T = 0.281 \text{ lb/sec/ft}$	$i_T q_T = 0.257 \text{ lb/sec/ft}$

The comparison between the two methods is quite good. The small discrepancies which occur after Step 8 in the sediment rate calculations are due to the use of different values for v_s in calculating the exponent z . The computer package uses the Rubey settling velocity equation to calculate v_s .

APPENDIX III - BED PROFILE COMPUTER MODEL

The bed profile model was described in Chapter 3, and a flow chart of the computer model was shown in Figure 3.4. The listings contained in this Appendix show that the bed profile model is actually used as a driving program for the sediment transport rate calculation package detailed in Appendix I.

The main program is used to read the input data and dynamically allocate core for the calculations. Subroutine DIVERGE generates the flow conditions and iterates until the proper flow depth corresponding to the specified flow and sediment transport rates is found.

The input data and card formats for the model are as follows:

Card 1	NS,SGS,D35,D65	(I10,3F10.0)
	NS	number of sediment size fractions
	SGS	specific gravity of the sediment
	D35	35 percent finer grain size (feet)
	D65	65 percent finer grain size (feet)
Card set 2	D,F	(2F10.0) NS cards
	D	grain diameter (feet)
	F	fraction of sediment mixture
Card 3	Wo,Wl	(2F10.0)
	coefficients of linear width variation	
	width = $W_o + W_l * (\text{distance into reservoir})$	
Card 4	NX,XSTART,DX,NT, NW ,Q,QTACT	(I10,6F10.0)
	NX	number of reservoir cross sections to be used
	XSTART	distance into reservoir of first cross section
	DX	distance between cross sections (feet)
	NT	Manning roughness coefficient for the total flow
	NW	Manning roughness coefficient for the reservoir walls
	Q	flow rate through reservoir (cfs)
	QTACT	actual total sediment load into reservoir (lb/sec)

The listing for the bed profile model follows. Comment cards have been used wherever necessary as an aid to the user.


```

C      PROGRAM SEDRES(INPUT,OUTPUT,TAPE5=INPUT,TAPE6=OUTPUT)
C
C      REAL NU,NT,NM
C      COMMON/TAPES/IR,IW
C      COMMON/E1/G,NU,RHO,GAMMA
C      COMMON/C1/W0,W1,SGS,D35,D65,ABAR,TOL
C      COMMON/C2/Q,NT,NM,DX,XSTART,QTACT
C      COMMON Z(1)
C
C      THIS ROUTINE SPECIFIES CORE STORAGE LOCATIONS FOR USE IN SUBROUTINE
C      DIVERG BY DYNAMIC ALLOCATION. THE NUMBER OF SAND SIZE FRACTIONS
C      ( NS ) AND NUMBER OF CROSS SECTIONS CALCULATED ( NX ) DETERMINE
C      THE AMOUNT OF CORE USED.
C      SPECIFY TOLERANCE FOR DEPTH ITERATION IN SUBROUTINE DIVERG
C      TOL=.005
C
C      READ(IR,1100)NS,SGS,D35,D65
C      NS      NUMBER OF SIZE FRACTIONS BEING USED
C      SGS      SPECIFIC GRAVITY OF THE SEDIMENT
C      D35      35 PERCENT FINER DIAMETER
C      D65      65 PERCENT FINER DIAMETER
C
C      ALLOCATE CORE SPACE FOR THE FOLLOWING ARRAYS -- NS WORDS PER ARRAY
C      D      SEDIMENT DIAMETER
C      F      SIZE FRACTION, PERCENT OF BED MATERIAL CORRESPONDING TO D
C      VS      SETTLING VELOCITY FOR PARTICLE OF DIAMETER D
C      BL      BED LOAD FOR D, POUNDS / SECOND / FOOT
C      TL      TOTAL LOAD FOR D, POUNDS / SECOND / FOOT
C
C      IF=1+NS
C      IVS=IF+NS
C      IBL=IVS+NS
C      ITL=IBL+NS
C      IX=ITL+NS
C      IEND=LOCF(Z(IX))
C      CALL REQMEM(IEND)
C
C      WRITE(IW,1540)SGS,D35,D65
C      DO 10 I=1,NS
C      READ(IR,1000)D,F
C      Z(I)=D
C      IEND=I+NS
C      Z(IEND)=F
C      CALL VSETTL(D,VS,SGS)
C      IEND=IEND+NS
C      Z(IEND)=VS
C      WRITE(IW,1545)D,F,VS
C
C      10 CONTINUE
C      READ COEFFICIENTS OF LINEAR WIDTH VARIATION
C      WIDTH = W0 + W1 * X
C      X      = DISTANCE FROM STARTING POINT AT WIDTH = W0
C
C      20 READ(IR,1000)W0,W1
C      CONTINUE
C      READ(IR,1100)NX,XSTART,DX,NT,NM,Q,QTACT
C      NX      NUMBER OF CROSS SECTIONS TO BE CALCULATED
C      XSTART  DISTANCE TO FIRST CROSS SECTION
C      DX      DISTANCE BETWEEN CROSS SECTIONS
C      NT      MANNING N FOR THE TOTAL FLOW
C      NM      MANNING N FOR THE WALLS
C      Q      FLOW RATE
C      QTACT   ACTUAL TOTAL LOAD THROUGH THE CROSS SECTIONS, WILL BE--
C              CONSTANT AT STEADY STATE
C
C      END OF FILE CHECK
C      IF (EOF(IR))40,30
C      ALLOCATE CORE SPACE FOR THE FOLLOWING ARRAYS -- NX WORDS PER ARRAY
C      X      DISTANCE FROM STARTING POINT ( DOWNSTREAM )
C      QB      TOTAL BED LOAD THROUGH THE CROSS SECTION, POUNDS / SECOND
C      QT      TOTAL SEDIMENT TRANSPORT THROUGH THE CROSS SECTION, LB / SEC
C      CA      BOTTOM CONCENTRATION OF THE SUSPENDED LOAD
C      DEEP    DEEP DEPTH AT THE CROSS SECTION
C
C      30 IQB=IX+NX
C      IQT=IQB+NX
C      IC=IQT+NX
C      IOP=IC+NX
C      IEND=LOCF(Z(IOP))+NX
C      CALL REQMEM(IEND)
C      PAGE EJECT

```

```

      WRITE(IW,1700)
      WRITE(IW,1570)Q,NT,NW
      CALL DIVERG(Z(I),Z(IF),Z(IVS),Z(IBL),Z(ITL),Z(IX),Z(IQB),Z(IQT),
2        Z(IC),Z(IDP),NX,NS)
C      REPEAT CALCULATIONS WITH NEXT SET OF FLOW DATA
      GO TO 20
40 STOP
1000 FORMAT(8F10.0)
1100 FORMAT(I10,7F10.0)
1540 FORMAT(2(/),10X,19HSEDIMENT PROPERTIES,/,30X,19HSPECIFIC GRAVITY =
2    ,F6.2,/,43X,6HD35 = ,E10.3,3H FT,/,43X,6HD65 = ,E10.3,3H FT,2(/),
331X,8HDIAMETER,8X,2HID,9X,2HVS,/)
1545 FORMAT(30X,E10.3,5X,F5.3,5X,E10.3)
1560 FORMAT(10X,16HWIDTH DEFINED BY,/,25X,4HW = ,E12.4,5H + ,E12.4,4H
2    * X,/)
1570 FORMAT(2(/),10X,12HFLOW RATE = ,F6.3,4H CFS,10X,13HMANNINGS N = ,F
25.3,15H FOR TOTAL FLOW,/,53X,2H= ,F5.3,10H FOR WALLS,2(/))
1700 FORMAT(1H1)
      END

```

```

SUBROUTINE DIVERG(D,F,VS,BL,TL,X,QB,QT,CA,DEEP,NX,NS)
  REAL NU,NT,NW
  NU = KINEMATIC VISCOSITY OF WATER, SPECIFIED IN BLOCK DATA OF SEDFLO
  NT = MANNING ROUGHNESS COEFFICIENT OF THE TOTAL FLOW
  NW = MANNING ROUGHNESS COEFFICIENT OF THE WALLS

  VARIABLE DIMENSION ARRAYS
  REAL D(NS),F(NS),VS(NS),BL(NS),TL(NS),X(NX),QB(NX),QT(NX),CA(NX)
  DEEP(NX)
  COMMON/TAPES/IR,IH
  COMMON/E1/G,NU,RHO,GAMMA
  COMMON/C1/W0,W1,SGS,035,065,ABAR,TOL
  COMMON/C2/Q,NT,NW,OX,XX,QTACT

  ITERATION TO FIND THE DEPTH OF FLOW SATISFYING THE TOTAL LOAD
  SPECIFIED. METHOD OF BISECTION IS USED -- IT IS ASSUMED THAT THE
  DEPTH IS LESS THAN 1 FOOT, TO MINIMIZE THE NUMBER OF ITERATIONS
  REQUIRED. IF GREATER DEPTHS ARE ANTICIPATED, D1 MAY BE CHANGED.

  DO 40 I=1,NX
    X(I)=XX
    W=W0+W1*XX
    N=0

  C SPECIFY UPPER AND LOWER LIMITS FOR DEPTH ITERATION
    D1=1.
    D2=.001
    DPTH=(D1+D2)/2.
  15 CONTINUE
    N=N+1

  C A MAXIMUM OF 50 ITERATIONS ARE ALLOWED
    IF(N.GT.50)GO TO 60
  C CALCULATE HYDRAULIC PARAMETERS FROM PHYSICAL DATA
    A=W*DPH
    WP=W+2.*DPH
    RT=A/WP
    U=Q/A
    R23=RT**0.66667
    SE=(U*NT/1.49/R23)**2
  C CALCULATE HYDRAULIC RADIUS WITH RESPECT TO THE BED (SEE EINSTEIN 1950)
    RW=(NW/NT*R23)**1.5
    RB=(A-2.*DPH*RW)/W

  C FIND BED AND TOTAL LOADS, AND RB PRIME FOR THIS DEPTH AND FIRST SIZE
    CALL SEDFLO(D(1),VS(1),U,SE,RB,RBP,DPH,035,065,SGS,T,E,0)

  C
    QT(1)=T*F(1)
    QB(1)=B*F(1)
    BL(1)=QB(1)
    TL(1)=QT(1)
    IF(NS.EQ.1)GO TO 30
  C RBP HAS BEEN CALCULATED FOR THE FIRST PARTICLE SIZE. USE ENTRY POINT
  C SEDRB FOR THE REST OF THE GRAIN SIZES.
    DO 20 J=2,NS
      CALL SEDRB (D(J),VS(J),U,SE,RB,RBP,DPH,035,065,SGS,T,E,0)
      BL(J)=B*F(J)
      TL(J)=T*F(J)
      QB(J)=QB(1)+BL(J)
      QT(J)=QT(1)+TL(J)
    20 CONTINUE
  30 CONTINUE

  C BW AND TW ARE THE BED AND TOTAL LOADS SUMMED FOR ALL SIZE FRACTIONS,
  C ON A UNIT WIDTH BASIS
    BW=QB(1)
    TW=QT(1)

  C MULTIPLY BY WIDTH TO FIND TOTAL RATES THROUGH CROSS SECTION
    QB(I)=QB(1)*W
    QT(I)=QT(1)*W

  C CHECK TO SEE IF CALCULATED QT IS CLOSE ENOUGH TO SPECIFIED TOTAL LOAD
    CHK=ABS((QTACT-QT(I))/QTACT)
    IF(CHK.LT.TOL)39,35
  C ADJUST DEPTH IN THE PROPER DIRECTION -- INCREASE OR DECREASE
  35 IF(QT(I).LT.QTACT)36,37
  36 D1=DPH
    DPTH=(DPH+D2)/2.
    GO TO 15
  37 D2=DPH

```

```

      OPTH=(OPTH+O1)/2.
      GO TO 15
39  DEEP(I)=OPTH
C    PRINT DATA FROM THIS CROSS SECTION
      WRITE(IW,1510)X(I),U,W,OPTH,SE,RT,RB,RBP
      DO 110 J=1,NS
      WRITE(IW,1520)O(J),BL(J),TL(J)
110  CONTINUE
      WRITE(IW,1530)BN,TW
C    MOVE ON TO THE NEXT CROSS SECTION
      XX=XX+OX
40  CONTINUE
C    PRINT SUMMARY OF ALL CROSS SECTIONS
      WRITE(IW,1540)
      DO 50 I=1,NX
      QS=QT(I)-OB(I)
      WRITE(IW,1550)X(I),QB(I),QS,QT(I),DEEP(I)
50  CONTINUE
      RETURN
60  STOP 1000
1510 FORMAT(3(/),5X,4HX = ,F4.1,3H FT,4X,4HU = ,F6.3 ,4X,4HW =
2, ,F5.2,4X,7HOPTH = ,F5.2,4X,5HSE = ,E10.3,4X,5HRT = ,F4.2,4X,5HRS =
3, ,F4.2,4X,6HRRBP = ,F4.2,2(/),33X,4HDIAN,12X,2HQB,13X,2HQT,/)
1520 FORMAT(30X,4(E10.3,5X))
1530 FORMAT(/,37X,5HTOTAL,3X,E10.3,5X,E10.3,2X,11HMB/(FT-SEC))
1540 FORMAT(5(/),10X,7HSUMMARY,5X,35H( BASED ON LB/SEC, NOT UNIT WIDTH
2),2(/),11X,1HX,12X,2HQB,13X,2HQS,13X,2HQT,11X,5HDEPTH,/)
1550 FORMAT(10X,F4.1,5(5X,E10.3))
      END

```

APPENDIX IV - RAW DATAAIV.1 Sediment Feed Rates

Average Flow Rate = 0.25 cfs

<u>Dry Weight of Sand</u>	<u>Time</u>	<u>Average Total Feed Rate</u>
24.06 lb	75 min	5.35×10^{-3}
16.00	45	5.93×10^{-3}
24.38	60	6.77×10^{-3}
<u>38.44</u>	<u>120</u>	<u>5.34×10^{-3}</u>
102.88 lb	300 min	$\bar{Q}_T = 5.72 \times 10^{-3} \text{ lb/sec}$

Average Flow Rate = 0.47 cfs

<u>Dry Weight of Sand</u>	<u>Time</u>	<u>Average Total Feed Rate</u>
56.69 lb	18.5 min	5.10×10^{-2}
57.19	15	6.35×10^{-2}
36.31	12	5.04×10^{-2}
34.81	12	4.83×10^{-2}
<u>46.94</u>	<u>20</u>	<u>3.91×10^{-2}</u>
231.94 lb	77.5 min	$\bar{Q}_T = 4.99 \times 10^{-2} \text{ lb/sec}$

AIV.2 Bedload Trap Data

Average Flow Rate = 0.25 cfs

Distance into Reservoir (ft)	Weight of Sand Accumulated (lb)	Time (min)	Bedload Rate (lb/sec/ft)
1.0	1.03	6	5.70×10^{-3}
	0.70	7	3.35×10^{-3}
	0.78	7	3.73×10^{-3}
	1.00	6	5.58×10^{-3}
	<u>0.62</u>	<u>6</u>	<u>3.47×10^{-3}</u>
	4.14	32	$\bar{q}_b = 4.31 \times 10^{-3}$ lb/ft/sec
(6 inch wide bedload trap)			
3.0	1.27	17	1.24×10^{-3}
	2.04	8	4.25×10^{-3}
	<u>1.85</u>	<u>16</u>	<u>1.93×10^{-3}</u>
	5.16	41	$\bar{q}_b = 2.10 \times 10^{-3}$ lb/sec/ft
5.0	2.00	15	2.22×10^{-3}
	1.22	15	1.36×10^{-3}
	1.68	15	1.86×10^{-3}
	1.44	15.5	1.55×10^{-3}
	<u>1.53</u>	<u>15</u>	<u>1.70×10^{-3}</u>
	7.87	75.5	$\bar{q}_b = 1.74 \times 10^{-3}$ lb/sec/ft

Distance into Reservoir (ft)	Weight of Sand Accumulated (lb)	Time (min)	Bedload Rate (lb/sec/ft)
7.0	1.65	15	1.83×10^{-3}
	1.62	15	1.80×10^{-3}
	1.63	9	3.03×10^{-3}
	1.63	15	1.81×10^{-3}
	<u>1.59</u>	<u>12</u>	<u>2.21×10^{-3}</u>
	8.12	66	$\bar{q}_b = 2.05 \times 10^{-3} \text{ lb/sec/ft}$

Average Flow Rate = 0.47 cfs

Distance into Reservoir (ft)	Weight of Sand Accumulated (lb)	Time (sec)	Bedload Rate (lb/sec/ft)
3.0	2.20	75	2.93×10^{-2}
	1.53	60	2.55×10^{-2}
	1.61	60	2.68×10^{-2}
	1.54	60	2.57×10^{-2}
	1.75	60	2.91×10^{-2}
	<u>1.90</u>	<u>66</u>	<u>3.16×10^{-2}</u>
	10.53	375	$\bar{q}_b = 2.81 \times 10^{-2} \text{ lb/ft/sec}$

Distance into Reservoir (ft)	Weight of Sand Accumulated (lb)	Time (sec)	Bedload Rate (lb/sec/ft)
5.0	1.39	90	1.55×10^{-2}
	1.88	60	3.13×10^{-2}
	2.57	90	2.86×10^{-2}
	1.43	60	2.39×10^{-2}
	2.46	60	4.10×10^{-2}
	<u>1.21</u>	<u>60</u>	<u>2.02×10^{-2}</u>
	10.95	420	$\bar{q}_b = 2.61 \times 10^{-2} \text{ lb/ft/sec}$

Distance into Reservoir (ft)	Weight of Sand Accumulated (lb)	Time (sec)	Bedload Rate (lb/sec/ft)
7.0	1.47	60	2.45×10^{-2}
	2.22	60	3.70×10^{-2}
	1.84	60	3.07×10^{-2}
	1.27	60	2.12×10^{-2}
	1.58	60	2.64×10^{-2}
	<u>0.98</u>	<u>60</u>	<u>1.64×10^{-2}</u>
	9.37	360	$\bar{q}_b = 2.60 \times 10^{-2} \text{ lb/ft/sec}$
9.0	1.63	120	1.36×10^{-2}
	2.13	90	2.36×10^{-2}
	1.61	75	2.15×10^{-2}
	1.62	75	2.16×10^{-2}
	1.15	75	1.54×10^{-2}
	<u>1.07</u>	<u>75</u>	<u>1.42×10^{-2}</u>
	9.21	510	$\bar{q}_b = 1.81 \times 10^{-2} \text{ lb/ft/sec}$
11.0	1.78	120	1.49×10^{-2}
	1.20	90	1.33×10^{-2}
	1.01	90	1.12×10^{-2}
	1.06	90	1.17×10^{-2}
	1.22	90	1.35×10^{-2}
	<u>0.83</u>	<u>90</u>	<u>0.92×10^{-2}</u>
	7.09	570	$\bar{q}_b = 1.24 \times 10^{-2} \text{ lb/ft/sec}$

AIV.3 Velocity, Turbulence Intensity, and Depth Data

The coordinate system used in taking velocity and turbulence intensity data is defined as follows:

- X Distance of cross section into the reservoir
- Y Distance from the left wall of the reservoir to the vertical on which measurements were taken
- Z Distance from water surface to the tip of the hot film probe.

The reduced data on the following pages are the results of the hot film annemometry studies performed in the laboratory reservoir at average flow rates of 0.25 and 0.47 cfs.

X (FT)	Y (FT)	Z (FT)	VELOCITY (FT/SEC)	TURBULENCE INTENSITY	AVERAGES FOR VELOCITY	VERTICAL TURB INT
0.0						
	.083					
		.154	1.284	.167		
		.537	1.513	.095		
		.835	1.559	.089		
					1.448	.118
	.250					
		.174	1.454	.107		
		.530	1.424	.108		
		.811	1.410	.097		
					1.430	.104
	.417					
		.280	1.353	.115		
		.633	1.311	.105		
		.839	1.353	.104		
					1.341	.109

AVERAGES FOR SECTION

VELOCITY	= 1.407 FT/SEC
TURBULENCE INTENSITY	= .111
FLOW RATE	= .25 CFS
DEPTH OF FLOW	= .357 FT

X (FT)	Y (FT)	Z (FT)	VELOCITY (FT/SEC)	TURBULENCE INTENSITY	AVERAGES FOR VERTICAL VELOCITY	VERTICAL TURB INT
1.5						
	.083					
		.123	1.311	.160		
		.342	1.410	.119		
		.561	1.410	.108		
		.781	1.395	.103		
					1.382	.121
	.250					
		.143	.724			
		.363	1.439	.129		
		.546	1.513	.085		
		.729	1.513	.079		
		.912	1.513	.074		
					1.299	.093
	.417					
		.144	.852	.263		
		.333	.927	.232		
		.523	1.102	.174		
		.712	1.381	.087		
		.902	1.395	.087		
					1.119	.173
	.583					
		.177	.506			
		.378	.906	.234		
		.578	1.102	.151		
		.779	1.191	.131		
					.926	.165

AVERAGES FOR SECTION

VELOCITY	= 1.141 FT/SEC
TURBULENCE INTENSITY	= .142
FLOW RATE	= .23 CFS
DEPTH OF FLOW	= .253 FT

X (FT)	Y (FT)	Z (FT)	VELOCITY (FT/SEC)	TURBULENCE INTENSITY	AVERAGES FOR VERTICAL VELOCITY	VERTICAL TURB INT
2.0						
	.083					
		.185	.377			
		.417	1.243			
		.648	1.367	.109		
		.833	1.367	.082		
					1.040	.094
	.250					
		.119	.389			
		.331	1.204	.136		
		.542	1.410	.070		
		.754	1.468	.053		
		.924	1.544	.058		
					1.170	.081
	.417					
		.149	1.191	.159		
		.415	1.367	.098		
		.681	1.395	.097		
		.894	1.454	.070		
					1.343	.109
	.583					
		.182	.950	.218		
		.429	1.191	.165		
		.675	1.395	.097		
		.921	1.454	.064		
					1.221	.144
	.750					
		.169	.287			
		.506	.984	.168		
		.843	1.066	.158		
					.775	.163

AVERAGES FOR SECTION

VELOCITY = 1.099 FT/SEC
 TURBULENCE INTENSITY = .120
 FLOW RATE = .20 CFS
 DEPTH OF FLOW = .203 FT

X (FT)	Y (FT)	Z (FT)	VELOCITY (FT/SEC)	TURBULENCE INTENSITY	AVERAGES FOR VELOCITY	VERTICAL TURB INT
2.5						
	.083					
		.172	1.178	.165		
		.437	1.498	.106		
		.834	1.559	.079		
					1.423	.114
	.250					
		.006	1.078	.193		
		.311	1.544	.105		
		.677	1.622	.104		
					1.509	.118
	.417					
		.067	1.140	.213		
		.250	1.529	.105		
		.494	1.606	.088		
		.799	1.702	.066		
					1.549	.104
	.583					
		.153	.895	.266		
		.379	.995	.269		
		.605	1.030	.296		
		.831	1.217	.209		
					1.039	.257
	.750					
		.164	.950			
		.429	1.042	.213		
		.746	1.297	.127		
					1.120	.163
	.917					
		.192	.225			
		.418	.873			
		.644	1.042	.106		
		.870	.972	.904		
					.738	.519

AVERAGES FOR SECTION

VELOCITY = 1.228 FT/SEC
 TURBULENCE INTENSITY = .184
 FLOW RATE = .20 CFS
 DEPTH OF FLOW = .170 FT

X (FT)	Y (FT)	Z (FT)	VELOCITY (FT/SEC)	TURBULENCE INTENSITY	AVERAGES FOR VELOCITY	VERTICAL TURB INT
3.0						
	.083					
		.130	1.243	.129		
		.379	1.367	.114		
		.689	1.424	.102		
					1.362	.112
	.250					
		.154	1.066	.194		
		.410	1.325	.176		
		.615	1.424	.129		
		.923	1.468	.101		
					1.310	.152
	.417					
		.093	.353			
		.324	1.018			
		.556	1.270	.156		
		.787	1.439	.118		
					1.076	.134
	.583					
		.169	.939	.231		
		.443	1.270	.167		
		.661	1.410	.119		
					1.231	.165
	.750					
		.137	.995			
		.423	1.297			
		.766	1.367	.120		
					1.241	.120
	.917					
		.134	.832	.265		
		.383	.724	.395		
		.632	1.165	.166		
		.881	1.217	.124		
					.982	.238

AVERAGES FOR SECTION

VELOCITY = 1.176 FT/SEC
 TURBULENCE INTENSITY = .168
 FLOW RATE = .24 CFS
 DEPTH OF FLOW = .189 FT

X (FT)	Y (FT)	Z (FT)	VELOCITY (FT/SEC)	TURBULENCE INTENSITY	AVERAGES FOR VELOCITY	VERTICAL TURB INT
3.5						
	.083					
		.164	.625			
		.481	1.066			
		.799	1.152	.132		
					.955	.132
	.250					
		.232	.415			
		.598	1.311	.143		
		.841	1.590	.094		
					1.018	.120
	.417					
		.286	.172			
		.557	1.325	.176		
		.818	1.606	.114		
					.926	.143
	.583					
		.082	1.284	.128		
		.422	1.468	.101		
		.762	1.622	.073		
					1.484	.096
	.750					
		.108	1.007	.155		
		.313	1.191	.136		
		.621	1.284	.139		
		.877	1.353	.109		
					1.219	.134
	.917					
		.144	.733			
		.451	.917	.264		
		.810	1.191	.119		
					.963	.188
	1.083					
		.094	.801	.179		
		.317	.961	.175		
		.650	1.090	.122		
		.872	1.204	.119		
					1.022	.148

AVERAGES FOR SECTION

VELOCITY = 1.072 FT/SEC
 TURBULENCE INTENSITY = .138
 FLOW RATE = .23 CFS
 DEPTH OF FLOW = .180 FT

X (FT)	Y (FT)	Z (FT)	VELOCITY (FT/SEC)	TURBULENCE INTENSITY	AVERAGES FOR VELOCITY	VERTICAL TURB INT
4.0						
	.083					
		.238	.852	.169		
		.619	.811	.216		
					.829	.196
	.250					
		.200	1.204	.124		
		.533	1.325	.093		
		.867	1.395	.092		
					1.302	.104
	.417					
		.286	.863			
		.524	1.204	.113		
		.802	1.311	.083		
					1.102	.096
	.583					
		.178	.724	.204		
		.474	.939	.189		
		.803	1.191	.113		
					.960	.166
	.750					
		.128	1.042	.136		
		.466	1.165	.126		
		.804	1.243	.090		
					1.157	.116
	.917					
		.210	.832			
		.532	1.018	.155		
		.855	1.284	.122		
					1.030	.139
	1.083					
		.225	.608			
		.408	.696			
		.638	.972	.133		
		.867	.984	.114		
					.803	.123

AVERAGES FOR SECTION

VELOCITY	=	.996 FT/SEC
TURBULENCE INTENSITY	=	.134
FLOW RATE	=	.20 CFS
DEPTH OF FLOW	=	.160 FT

X (FT)	Y (FT)	Z (FT)	VELOCITY (FT/SEC)	TURBULENCE INTENSITY	AVERAGES FOR VELOCITY	VERTICAL TURB INT
4.5						
	.083					
		.301	1.102			
		.496	1.353	.098		
		.797	1.325	.066		
					1.243	.079
	.250					
		.240	1.066	.152		
		.421	1.165	.120		
		.772	1.270	.095		
					1.175	.120
	.417					
		.161	.103	.359		
		.379	1.127	.144		
		.616	1.270	.117		
		.853	1.339	.110		
					.940	.186
	.583					
		.291	1.325	.126		
		.627	1.544	.095		
		.851	1.513	.095		
					1.435	.109
	.750					
		.313	.972			
		.641	1.367	.147		
		.894	1.454	.112		
					1.199	.132
	.917					
		.435	1.339			
		.797	1.339	.132		
					1.339	.132
	1.083					
		.237	1.297	.105		
		.596	1.270	.089		
		.885	1.257	.095		
					1.278	.097
	1.250					
		.367	.762			
		.620	1.191	.113		
		.810	1.165	.074		
					.972	.091

AVERAGES FOR SECTION

VELOCITY	= 1.176 FT/SEC
TURBULENCE INTENSITY	= .125
FLOW RATE	= .26 CFS
DEPTH OF FLOW	= .162 FT

X (FT)	Y (FT)	Z (FT)	VELOCITY (FT/SEC)	TURBULENCE INTENSITY	AVERAGES FOR VELOCITY	VERTICAL TURB INT
5.0						
	.083					
		.308	.625			
		.769	1.653	.093	1.100	.093
	.250					
		.400	1.622	.104		
		.634	1.836	.080		
		.876	1.870	.070	1.733	.090
	.417					
		.203	1.030			
		.772	1.544	.105	1.293	.105
	.583					
		.163	1.178			
		.556	1.529	.116		
		.817	1.622	.099	1.432	.108
	.750					
		.280	1.339			
		.753	1.686	.134	1.507	.134
	.917					
		.122	1.115	.186		
		.439	1.152	.218		
		.793	1.559	.137	1.298	.178
	1.083					
		.291	1.325	.182		
		.528	1.513	.148		
		.843	1.622	.109	1.470	.150
	1.250					
		.255	.428			
		.453	.832			
		-.161	1.127	.220		
		.880	1.152	.172	.957	.184

AVERAGES FOR SECTION

VELOCITY = 1.301 FT/SEC
 TURBULENCE INTENSITY = .143
 FLOW RATE = .30 CFS
 DEPTH OF FLOW = .159 FT

X (FT)	Y (FT)	Z (FT)	VELOCITY (FT/SEC)	TURBULENCE INTENSITY	AVERAGES FOR VELOCITY	VERTICAL TURB INT
5.5						
	.083					
		.353	1.217			
		.774	1.498	.117		
					1.340	.117
	.250					
		.205	.984	.247		
		.548	1.230	.220		
		.822	1.468	.166		
					1.212	.213
	.417					
		.329	1.325			
		.800	1.606	.120		
					1.447	.120
	.583					
		.316	1.030	.226		
		.719	1.637	.124		
					1.323	.177
	.750					
		.389	1.217	.170		
		.786	1.468	.139		
					1.321	.157
	.917					
		.249	1.230	.180		
		.491	1.339	.170		
		.855	1.559	.105		
					1.371	.153
	1.083					
		.426	1.367	.142		
		.659	1.575	.115		
		.886	1.606	.099		
					1.469	.126
	1.250					
		.284	1.042			
		.606	1.311	.155		
		.929	1.513	.101		
					1.238	.132
	1.417					
		.218	1.165			
		.570	1.410	.108		
		.923	1.439	.102		
					1.321	.106

AVERAGES FOR SECTION

VELOCITY	= 1.343 FT/SEC
TURBULENCE INTENSITY	= .149
FLOW RATE	= .31 CFS
DEPTH OF FLOW	= .148 FT

X (FT)	Y (FT)	Z (FT)	VELOCITY (FT/SEC)	TURBULENCE INTENSITY	AVERAGES FOR VERTICAL VELOCITY	VERTICAL TURB INT
6.0						
	.083					
		.150	1.230	.175		
		.515	1.178	.154		
					1.195	.161
	.250					
		.353	1.054	.195		
		.699	1.140	.196		
					1.095	.195
	.417					
		.316	.972	.211		
		.632	1.115	.180		
		.842	1.297	.133		
					1.095	.183
	.583					
		.324	.873			
		.598	1.230			
		.882	1.513			
					1.139	
	.750					
		.534	1.454			
					1.454	
	.917					
		.013	1.454	.139		
		.467	1.424	.119		
		.707	1.468	.107		
					1.450	.119
	1.083					
		.350	1.529	.164		
		.742	1.590	.115		
					1.557	.142
	1.250					
		.307	1.191	.148		
		.542	.873	.137		
		.838	1.590	.099		
					1.230	.130
	1.417					
		.352	1.127			
		.610	1.339	.121		
		.799	1.454	.107		
					1.271	.113

AVERAGES FOR SECTION

VELOCITY = 1.254 FT/SEC
 TURBULENCE INTENSITY = .148
 FLOW RATE = .28 CFS
 DEPTH OF FLOW = .138 FT

X (FT)	Y (FT)	Z (FT)	VELOCITY (FT/SEC)	TURBULENCE INTENSITY	AVERAGES FOR VELOCITY	VERTICAL TURB INT
6.5	.083	.342 .610 .801	1.165 1.102 1.127	.155 .175 .179		
	.250	.162 .469 .792	1.257 1.284 1.439	.134 .156 .118	1.140	.166
	.417	.219 .461 .797	.733 1.018 1.410	.346 .173	1.333	.135
	.583	.233 .500	.687 1.686	.113	1.067	.249
	.750	.271 .542 .822	1.204 1.367 1.529	.159 .142 .116	1.319	.113
	.917	.238 .600 .872	1.054 1.590 1.751	.271 .152 .112	1.352	.141
	1.083	.167 .508 .826	1.054 1.529 1.622	.164 .125	1.395	.194
	1.250	.455 .736 .874	.660 .884 1.217	.400 .323 .237	1.400	.144
	1.417	.247 .478 .731 .918	.216 .506 1.395 1.367	.163 .131	.816	.352
	1.583	.323 .669 .880	.207 1.078 1.127		.748	.149
					.643	

AVERAGES FOR SECTION

VELOCITY	=	1.063	FT/SEC
TURBULENCE INTENSITY	=	.203	
FLOW RATE	=	.26	CFS
DEPTH OF FLOW	=	.143	FT

X (FT)	Y (FT)	Z (FT)	VELOCITY (FT/SEC)	TURBULENCE INTENSITY	AVERAGES VELOCITY	FOR VERTICAL TURB INT
7.0						
	.083					
		.218	1.339	.165		
		.511	1.090	.234		
		.759	1.178	.229		
					1.213	.207
	.250					
		.500	1.311	.177		
		.825	1.622	.114		
					1.416	.156
	.416					
		.236	1.410	.108		
		.545	1.653	.098		
		.772	1.686	.082		
					1.569	.097
	.583					
		.303	.811	.332		
		.555	1.575	.126		
		.773	1.785	.086		
					1.318	.201
	.750					
		.348	.544			
		.775	1.637	.104		
					1.023	.104
	.916					
		.757	1.559	.105		
					1.559	.105
	1.083					
		.500	1.498	.107		
					1.498	.107
	1.249					
		.368	1.030	.178		
		.776	.906	.216		
					.977	.195
	1.416					
		.339	.195			
		.589	1.284			
		.833	1.637			
					.881	
	1.583					
		.454	.863			
		.840	1.270	.157		
					1.007	.157
	1.749					
		.417	1.007			
					1.007	

AVERAGES FOR SECTION

VELOCITY = 1.222 FT/SEC
 TURBULENCE INTENSITY = .147
 FLOW RATE = .32 CFS
 DEPTH OF FLOW = .142 FT

X (FT)	Y (FT)	Z (FT)	VELOCITY (FT/SEC)	TURBULENCE INTENSITY	AVERAGES VELOCITY	FOR VERTICAL TURB INT
7.5	.083	0.000 .631	.660 .939	.299 .257		
	.250	.417 .778	1.243 1.381	.169 .185	.851	.270
	.416	.226 .678	.575 .939	.330	1.299	.176
	.583	.274 .698	1.243 1.670	.146 .113	.774	.330
	.750	.316 .673	.435 1.735	.385 .153	1.462	.129
	.916	.111 .648	.521 1.498	.160	1.891	.268
	1.083	.244 .733	1.217 1.498	.125 .128	1.127	.160
	1.249	.141 .739	1.257 1.544	.123 .148	1.361	.126
	1.416	.169 .471 .816	.371 1.353 1.590	.154 .099	1.417	.137
	1.583	.163 .429 .769	.863 1.127 1.498	.188 .209 .128	1.123	.125
	1.749	.173 .469 .784	.220 1.243 1.575	.169 .089	1.198	.170
	1.916	.753 .472 .129	.852 1.297 1.284	.133 .123	1.839	.125
					1.015	.114

AVERAGES FOR SECTION

VELOCITY = 1.147 FT/SEC
 TURBULENCE INTENSITY = .184
 FLOW RATE = .23 CFS
 DEPTH OF FLOW = .103 FT

X (FT)	Y (FT)	Z (FT)	VELOCITY (FT/SEC)	TURBULENCE INTENSITY	AVERAGES VELOCITY	FOR VERTICAL TURB INT
8.0	.083	.409 .727	.762 .552	.189 .236		
	.250	.246 .607	.642 1.339	.165	.671	.209
	.417	.305 .589 .815	1.270 1.243 1.454	.157 .180 .140	1.042	.165
	.583	.206 .581 .816	.402 1.152 1.483	.253 .160	1.318	.158
	.750	.227 .588 .784	1.513 1.653 1.559	.112 .114 .116	.957	.207
	.917	.212 .525 .768	1.483 1.468 1.410	.171 .118 .119	1.567	.113
	1.083	.023 .337 .628	1.339 1.243 1.217	.182 .270 .294	1.453	.138
	1.250	.315 .449 .719	.906 1.007 1.066	.272 .311 .318	1.247	.267
	1.417	.009 .536 .741	1.090 1.257 1.217	.164 .168 .147	.993	.299
	1.583	.209 .687	1.284 1.410	.139 .130	1.197	.159
	1.750	.157 .652	.791 1.007	.204	1.353	.134
	1.917	.226 .491 .755	1.030 1.204 1.353	.121	.920	.204
					1.198	.121

AVERAGES FOR SECTION

VELOCITY = 1.155 FT/SEC
 TURBULENCE INTENSITY = .181
 FLOW RATE = .25 CFS
 DEPTH OF FLOW = .106 FT

X (FT)	Y (FT)	Z (FT)	VELOCITY (FT/SEC)	TURBULENCE INTENSITY	AVERAGES FOR VELOCITY	VERTICAL TURB INT
2.0						
	.083					
		.148	2.378	.101		
		.542	2.716	.053		
		.887	3.037	.043		
					2.691	.067
	.250					
		.126	2.200	.118		
		.480	2.783	.057		
		.833	2.943	.043		
					2.661	.071
	.417					
		.098	2.317	.112		
		.478	2.806	.048		
		.859	2.874	.044		
					2.687	.065
	.583					
		.138	2.357	.120		
		.511	2.586	.063		
		.883	2.806	.048		
					2.578	.077
	.750					
		.241	2.522	.109		
		.494	2.564	.059		
		.810	2.607	.054		
					2.564	.075

AVERAGES FOR SECTION

VELOCITY = 2.636 FT/SEC
 TURBULENCE INTENSITY = .071
 FLOW RATE = .43 CFS
 DEPTH OF FLOW = .185 FT

X (FT)	Y (FT)	Z (FT)	VELOCITY (FT/SEC)	TURBULENCE INTENSITY	AVERAGES FOR VELOCITY	VERTICAL TURB INT
3.0						
	.083					
		.256	2.378	.083		
		.694	2.480	.064		
					2.431	.073
	.250					
		.302	2.586	.081		
		.716	2.694	.049		
					2.639	.065
	.417					
		.301	2.278	.131		
		.723	2.564	.072		
					2.418	.102
	.583					
		.329	2.629	.090		
		.741	2.828	.048		
					2.721	.071
	.750					
		.337	2.543	.113		
		.751	2.783	.053		
					2.652	.086
	.917					
		.389	2.629	.099		
		.778	2.874	.044		
					2.731	.076

AVERAGES FOR SECTION

VELOCITY = 2.612 FT/SEC
 TURBULENCE INTENSITY = .079
 FLOW RATE = .48 CFS
 DEPTH OF FLOW = .170 FT

X (FT)	Y (FT)	Z (FT)	VELOCITY (FT/SEC)	TURBULENCE INTENSITY	AVERAGES FOR VELOCITY	FOR VERTICAL TURB INT
4.0						
	.083					
		.240	2.357	.125		
		.628	2.851	.070		
					2.637	.094
	.250					
		.270	2.966	.096		
		.541	3.061	.052		
					3.022	.069
	.417					
		.260	2.522	.132		
		.603	2.851	.062		
					2.709	.092
	.583					
		.265	2.650	.121		
		.605	3.109	.056		
					2.909	.084
	.750					
		.281	2.874	.096		
		.640	3.157	.051		
					3.027	.072
	.917					
		.276	3.013	.073		
		.649	3.231	.042		
					3.130	.057
	1.083					
		.271	2.543	.100		
		.659	3.133	.051		
					2.859	.074

AVERAGES FOR SECTION

VELOCITY	= 2.898 FT/SEC
TURBULENCE INTENSITY	= .077
FLOW RATE	= .51 CFS
DEPTH OF FLOW	= .138 FT

X (FT)	Y (FT)	Z (FT)	VELOCITY (FT/SEC)	TURBULENCE INTENSITY	AVERAGES FOR VELOCITY	VERTICAL TURB INT
5.0						
	.083					
		.276	2.278	.131		
		.621	2.990	.069		
					2.671	.097
	.250					
		.294	2.761	.106		
		.784	3.061	.043		
					2.899	.077
	.417					
		.257	2.761	.111		
		.624	2.920	.061		
					2.850	.083
	.583					
		.297	2.501	.100		
		.658	3.231	.042		
					2.882	.070
	.750					
		.200	2.543	.100		
		.564	2.920	.065		
					2.776	.079
	.917					
		.336	2.258	.127		
		.641	2.650	.081		
					2.459	.103
	1.083					
		.234	2.439	.110		
		.547	3.085	.052		
					2.832	.074
	1.250					
		.309	2.629	.094		
		.673	3.157	.043		
					2.898	.068

AVERAGES FOR SECTION

VELOCITY = 2.785 FT/SEC
 TURBULENCE INTENSITY = .081
 FLOW RATE = .46 CFS
 DEPTH OF FLOW = .114 FT

X (FT)	Y (FT)	Z (FT)	VELOCITY (FT/SEC)	TURBULENCE INTENSITY	AVERAGES VELOCITY	FOR VERTICAL TURB INT
6.0						
	.083					
		.317	2.161	.143		
		.798	2.738	.067		
					2.417	.109
	.250					
		.270	2.586	.104		
		.721	3.013	.047		
					2.801	.075
	.417					
		.257	2.501	.109		
		.699	2.966	.065		
					2.744	.086
	.583					
		.295	2.564	.095		
		.771	3.037	.052		
					2.785	.075
	.750					
		.252	2.238	.122		
		.738	2.761	.080		
					2.502	.101
	.917					
		.326	2.851	.088		
		.642	3.133	.102		
					2.996	.095
	1.083					
		.340	2.067			
		.825	3.256	.059		
					2.563	.059
	1.250					
		.277	2.629	.108		
		.772	3.013	.065		
					2.812	.087
	1.417					
		.297	2.439	.128		
		.792	2.990	.052		
					2.690	.094

AVERAGES FOR SECTION

VELOCITY = 2.699 FT/SEC
 TURBULENCE INTENSITY = .089
 FLOW RATE = .46 CFS
 DEPTH OF FLOW = .104 FT

X (FT)	Y (FT)	Z (FT)	VELOCITY (FT/SEC)	TURBULENCE INTENSITY	AVERAGES VELOCITY	FOR VERTICAL TURB INT
7.0						
	.083					
		.337	2.180	.133		
		.699	2.806	.070		
					2.482	.103
	.250					
		.226	2.278	.112		
		.583	2.897	.074		
					2.646	.090
	.417					
		.259	2.357	.120		
		.753	3.085	.060		
					2.717	.091
	.583					
		.283	2.142	.133		
		.609	2.897	.052		
					2.561	.088
	.750					
		.198	2.357	.107		
		.594	2.738	.080		
					2.587	.090
	.917					
		.242	2.418	.120		
		.663	2.874	.070		
					2.668	.092
	1.083					
		.196	2.337	.130		
		.608	2.920	.061		
					2.686	.089
	1.250					
		.316	2.317	.112		
		.737	3.133	.043		
					2.704	.079
	1.417					
		.289	2.501	.105		
		.651	2.738	.080		
					2.627	.092
	1.583					
		.271	2.378	.139		
		.792	3.109	.043		
					2.720	.094

AVERAGES FOR SECTION

VELOCITY = 2.648 FT/SEC
 TURBULENCE INTENSITY = .091
 FLOW RATE = .44 CFS
 DEPTH OF FLOW = .091 FT

X (FT)	Y (FT)	Z (FT)	VELOCITY (FT/SEC)	TURBULENCE INTENSITY	AVERAGES VELOCITY	FOR VERTICAL TURB INT
8.0	.083	.220 .674	1.819 2.738	.220 .076		
	.250	.321 .691	2.672 2.920	.098 .070	2.327	.140
	.417	.291 .583	2.378 2.522	.111 .137	2.794	.084
	.583	.244 .569	2.398 3.281	.148 .051	2.459	.125
	.750	.385	2.806	.106	2.922	.090
	.917	.312 .688	2.238 2.378	.141 .102	2.806	.106
	1.083	.333 .678	2.278 2.543	.150 .100	2.308	.122
	1.250	.390 .756	2.459 2.897	.110 .074	2.409	.125
	1.417	.333 .778	2.200 2.607	.123 .099	2.646	.095
	1.583	.381 .691	2.480 2.629	.101 .081	2.381	.112
	1.750	.431 .725	2.123 2.439	.172 .110	2.549	.091
	1.917	.390 .779	1.888 2.522	.188 .077	2.256	.146
					2.151	.142

AVERAGES FOR SECTION

VELOCITY = 2.474 FT/SEC
 TURBULENCE INTENSITY = .118
 FLOW RATE = .51 CFS
 DEPTH OF FLOW = .101 FT

X (FT)	Y (FT)	Z (FT)	VELOCITY (FT/SEC)	TURBULENCE INTENSITY	AVERAGES FOR VELOCITY	VERTICAL TURB INT
9.0						
	.083	.353 .706	1.958 2.398	.147 .102		
	.250	.385 .769	2.200 2.716	.147 .085	2.165	.126
	.417	.318 .671	1.976 2.851	.171 .092	2.418	.121
	.583	.346 .716	2.105 2.522	.154 .100	2.419	.131
	.750	.318 .659	2.200 2.650	.161 .090	2.300	.128
	.917	.305 .671	1.870 2.650	.238 .090	2.430	.125
	1.083	.296 .718	2.378 2.806	.139 .097	2.270	.162
	1.250	.474 .868	2.378 2.607	.130 .108	2.588	.118
	1.417	.293 .693	1.940 2.439	.177 .110	2.453	.123
	1.583	.351 .702	2.278 2.607	.136 .135	2.193	.143
	1.750	.443 .753	2.297 2.418	.122 .106	2.434	.136
	1.917	.333 .778	1.940 2.459	.147 .105	2.346	.115
					2.171	.129

AVERAGES FOR SECTION

VELOCITY	=	2.330	FT/SEC
TURBULENCE INTENSITY	=	.130	
FLOW RATE	=	.44	CFS
DEPTH OF FLOW	=	.086	FT

X (FT)	Y (FT)	Z (FT)	VELOCITY (FT/SEC)	TURBULENCE INTENSITY	AVERAGES VELOCITY	FOR VERTICAL TURB INT
10.0						
	.167					
		.268	1.544	.189		
		.625	2.086	.120		
					1.844	.151
	.500					
		.317	1.958	.176		
		.635	2.219	.132		
					2.095	.153
	.833					
		.319	1.353			
		.745	1.923	.147		
					1.620	.147
	1.167					
		.364	2.123	.124		
		.667	2.238	.141		
					2.179	.132
	1.500					
		.308	1.802	.150		
		.769	2.278	.107		
					2.021	.130
	1.833					
		.364	1.637	.185		
		.788	1.976	.107		
					1.781	.152
	2.167					
		.313	1.768	.156		
		.729	2.031	.106		
					1.894	.132

AVERAGES FOR SECTION

VELOCITY	= 1.901 FT/SEC
TURBULENCE INTENSITY	= .142
FLOW RATE	= .42 CFS
DEPTH OF FLOW	= .093 FT

X (FT)	Y (FT)	Z (FT)	VELOCITY (FT/SEC)	TURBULENCE INTENSITY	AVERAGES FOR VELOCITY	VERTICAL TURB INT
11.0						
	.167					
		.307	1.735	.163		
		.302	1.302	.151		
					1.765	.157
	.500					
		.800	1.751	.162		
					1.751	.162
	.833					
		.313	1.958	.162		
		.729	2.180	.123		
					2.065	.143
	1.167					
		.306	1.958	.157		
		.714	2.398	.129		
					2.174	.143
	1.500					
		.348	1.702	.139		
		.783	2.067	.135		
					1.861	.166
	1.833					
		.326	1.958	.123		
		.652	2.219	.132		
					2.091	.128
	2.167					
		.379	1.529	.242		
		.724	2.012	.126		
					1.745	.190
	2.500					
		.279	1.686	.164		
		.628	1.718	.143		
					1.704	.152

AVERAGES FOR SECTION

VELOCITY	= 1.895 FT/SEC
TURBULENCE INTENSITY	= .157
FLOW RATE	= .50 CFS
DEPTH OF FLOW	= .101 FT

APPENDIX V - VELOCITY AND TURBULENCE INTENSITY RELATIONSHIPS

Plots showing the variation and turbulence intensity with distance into the reservoir for both experimental flow rates are shown in Figures AV.1 and AV.2. The curves were constructed using data taken with the hot film anemometry unit during the experimental testing (see section 4.1.5 and Appendix IV).

For an average flow rate of 0.25 cfs, the velocity remained nearly constant over the length of the steady state region. The turbulence intensity of the flow was somewhat scattered, as would be expected due to the presence of well developed bed forms, but there seems to be a trend of increasing turbulence intensity with distance into the reservoir.

At an average flow rate of 0.47 cfs with a plane bed in the steady state region, there is a smooth decrease in velocity with distance into the reservoir, as shown by Figure AV.2. The two points near the entrance of the reservoir that do not fall on the curve are probably due to local scour. The turbulence intensity of the flow shows a smoothly increasing trend with distance into the reservoir.

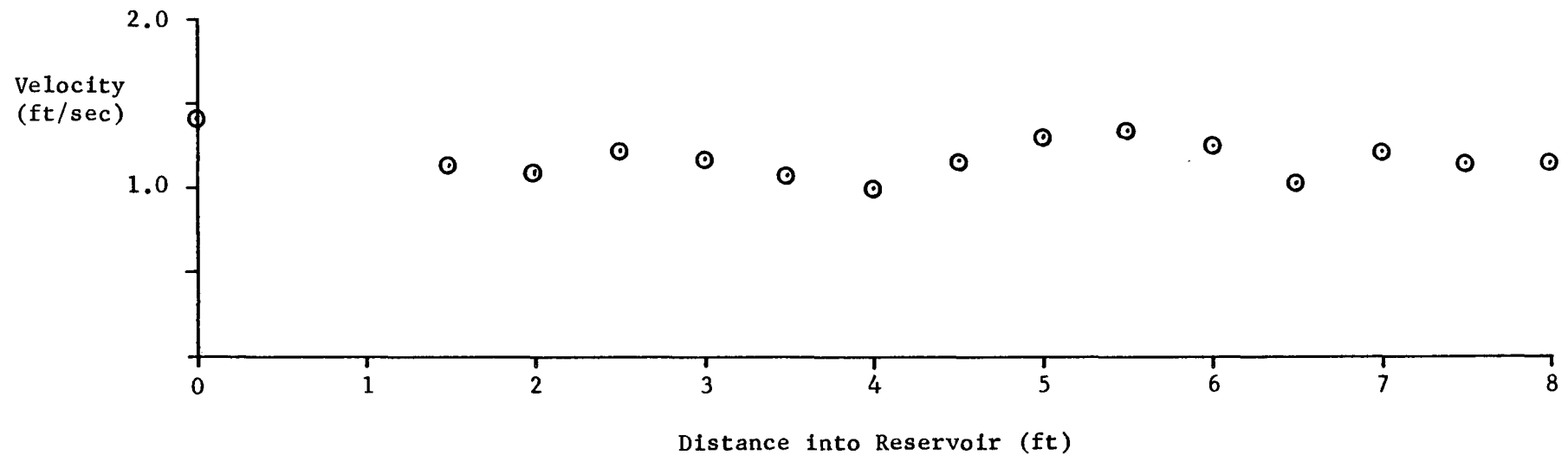
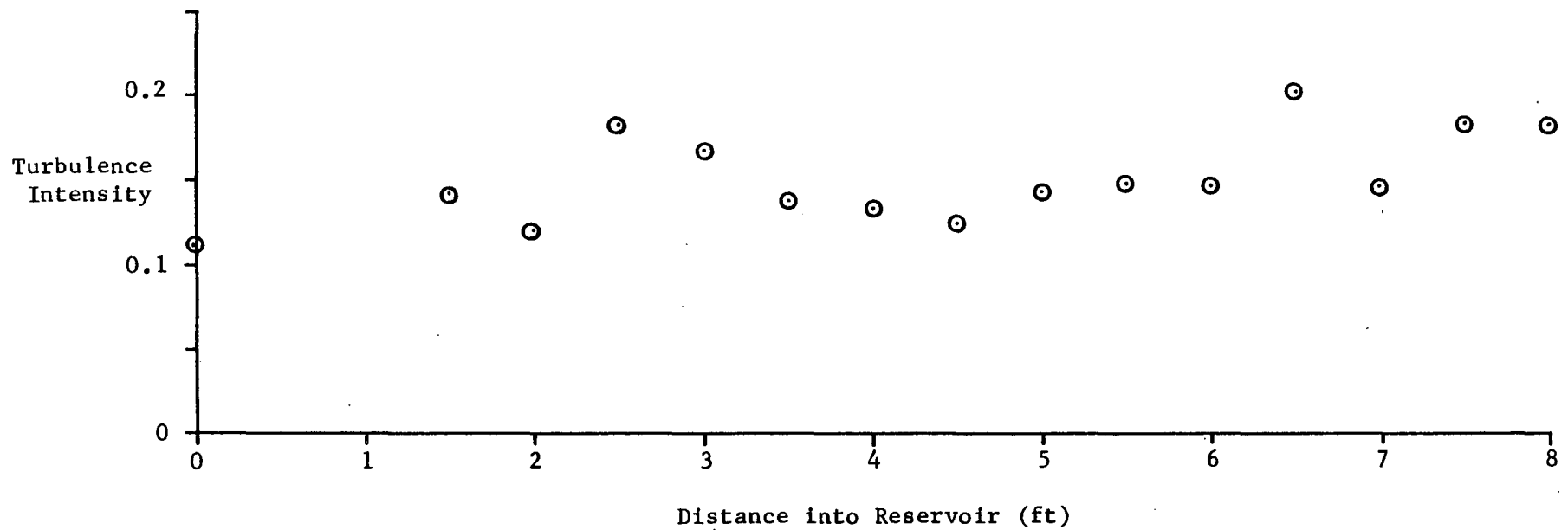


Figure AV.1 Velocity and Turbulence Intensity
Flow Rate = 0.25 cfs

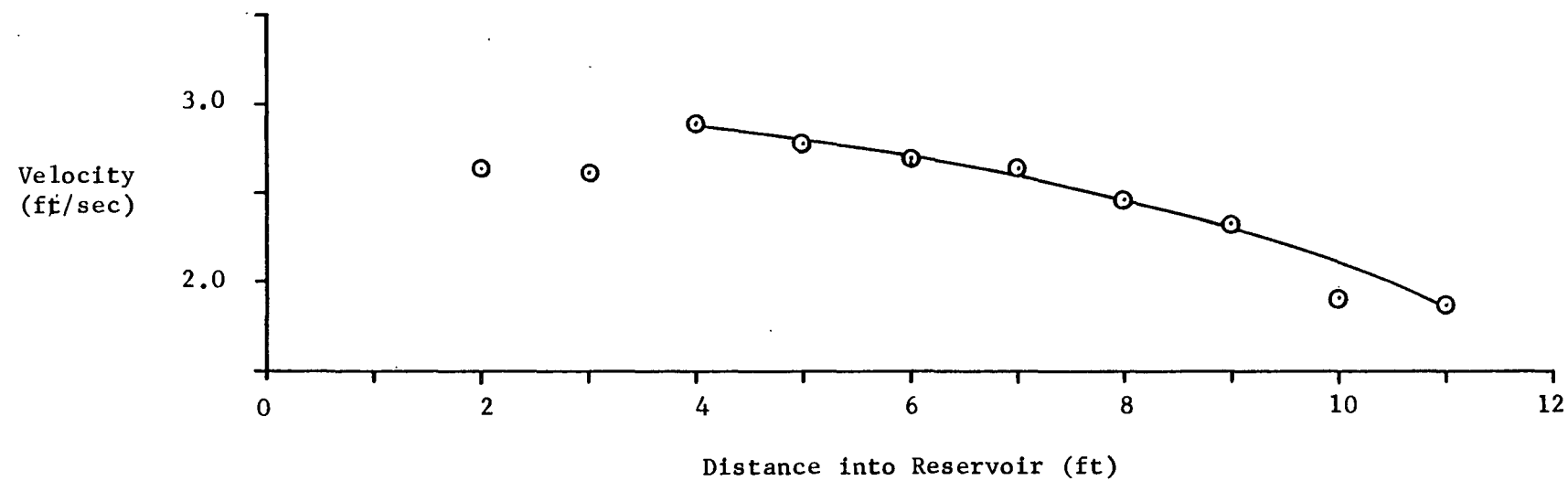
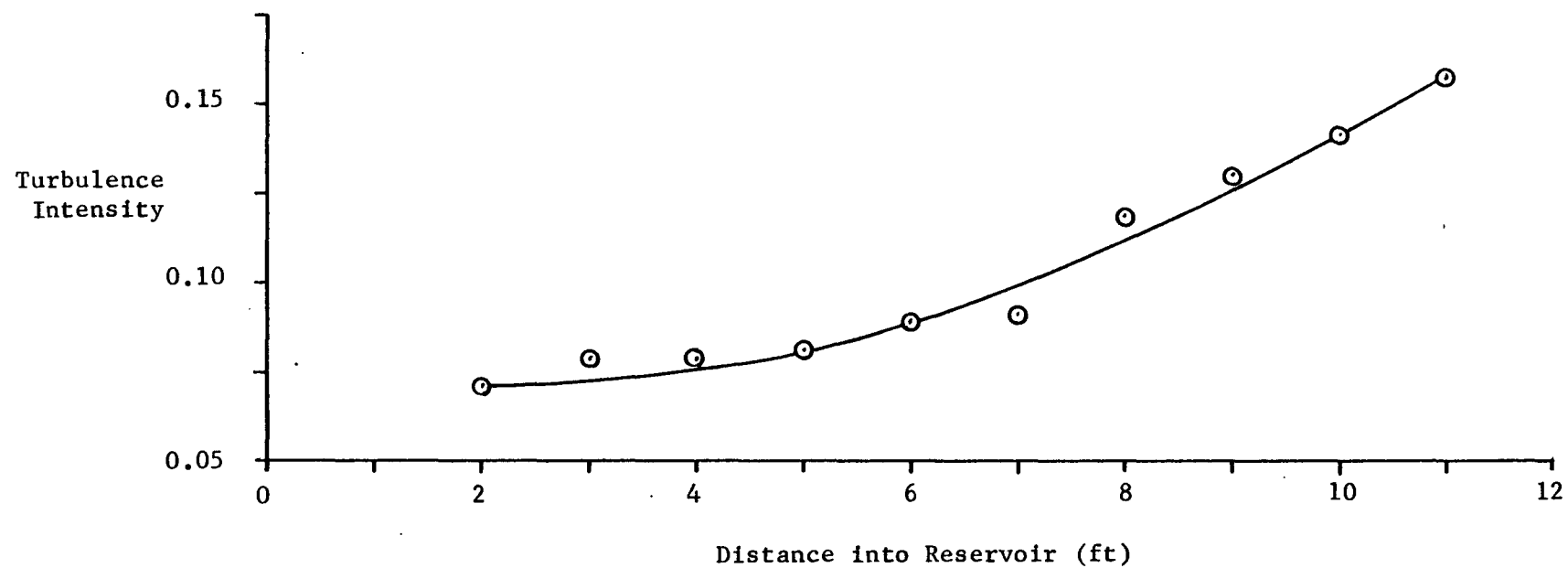


Figure AV.2 Velocity and Turbulence Intensity
Flow Rate = 0.47 cfs

VITA

David C. Beechwood was born in Abington, Pennsylvania, on June 17, 1954. He grew up in Huntingdon Valley, Pennsylvania, and graduated from Lower Moreland High School in 1972.

The author enrolled at Lehigh University where he became a member of Tau Beta Pi. He graduated in 1976 with a Bachelor of Science degree in Civil Engineering. He then entered a Master of Science program in the Water Resources Division of the Civil Engineering Department at Lehigh, and graduated in 1978. During his graduate work he was a Research Assistant and a Teaching Assistant.